N-substituted benzimidazole acrylonitriles as *in vitro* tubulin polymerization inhibitors: synthesis, biological activity and computational analysis

N. Perin[1‡], L. Hok[2‡], A. Beč[1], L. Persoons[3], E. Vanstreels[3], D. Daelemans[3],
R. Vianello[2]* and M. Hranjec[1]*

[1] Department of Organic Chemistry, Faculty of Chemical Engineering and Technology, University of Zagreb, Marulićev trg 19, HR-10000 Zagreb, Croatia
[2] Division of Organic Chemistry and Biochemistry, Ruđer Bošković Institute, Bijenička cesta 54, HR-10000 Zagreb, Croatia
[3] KU Leuven Department of Microbiology, Immunology and Transplantation, Laboratory of Virology and Chemotherapy, Rega Institute, Leuven, Belgium

[‡] These authors have contributed equally.

[*] Corresponding authors: Dr. Marijana Hranjec, Full. Prof., Department of Organic Chemistry, Faculty of Chemical Engineering and Technology, University of Zagreb, Marulićev trg 19, P.O. Box 177, HR-10000 Zagreb, Croatia, Phone No. +385-1-4597245; Fax No. +385-1-4597250; e-mail: mhranjec@fkit.hr

Dr. Robert Vianello, Division of Organic Chemistry and Biochemistry, Ruđer Bošković Institute, Bijenička cesta 54, HR-10000 Zagreb, Croatia; e-mail: Robert.Vianello@irb.hr

Abstract

We present the design, synthesis and biological activity of novel *N*-substituted benzimidazole based acrylonitriles as potential inhibitors of the tubulin polymerization. Their synthesis was achieved using classical linear organic and microwave assisted techniques, starting from aromatic aldehydes and *N*-substituted-2-cyanomethylbenzimidazoles. All newly prepared compounds were tested for their antiproliferative activity *in vitro* on eight human cancer cell lines and one reference non-cancerous assay. *N,N*-dimethylamino substituted acrylonitriles **30** and **41**, bearing *N*-isobutyl and cyano substituents placed on the benzimidazole nuclei, showed strong and selective antiproliferative activity in the submicromolar range of inhibitory concentrations (IC$_{50}$ 0.2 – 0.6 μM), while being significantly less toxic than reference systems docetaxel and staurosporine, thus promoting them as lead compounds. Mechanism of action studies demonstrated that two most active compounds inhibited the polymerization of tubulin. Computational analysis confirmed the suitability of the employed benzimidazole-acrylonitrile skeleton for the binding within the colchicine binding site in tubulin, thus rationalizing the observed antitumor activities, and demonstrated that *E*-isomers are active substances. It also provided structural determinants affecting both the binding position and the matching affinities, identifying the attached NMe$_2$ group as the most dominant in promoting the binding, which allows ligands to optimize favorable cation$\cdots\pi$ and hydrogen bonding interactions with Lys352.

1. Introduction

Due to their widespread applications and interesting chemical, biological and pharmacological features, benzimidazoles have been an important subject of intensive investigations in organic and medicinal chemistry in recent years [1,2]. Benzimidazole scaffold, as a small nitrogen-containing heterocycle, has become an important and fundamental building block widely incorporated in the structure of numerous natural and synthetic molecules displaying versatile biological activities [3,4]. The fact that benzimidazole nuclei are bio-isosters of naturally occurring purine is of great importance, since benzimidazole derivatives play a crucial role in the function of many biologically important molecules due to their interaction with DNA, RNA or different proteins [5,6]. Previously, we have shown that benzimidazole derivatives are an important structural motif of small heterocyclic molecules possessing promising and strong antiproliferative activity in submicromolar range of inhibitory concentrations with observed selectivity towards some cancer cells [7,8]. For example, we have demonstrated that various amidino- and cyano substituted styryl-2-benzimidazoles and benzimidazo[1,2-*a*]quinolones showed strong inhibitory activities on several human cell lines [9,10]. Furthermore, the antiproliferative activity was strongly enhanced by the cyano substituent, allowing benzimidazo[1,2-*a*]quinoline-9(10)-carbonitrile derivatives to show pronounced and selective activity on HeLa cells (IC_{50} = 0.05 μM). Additionally, benzimidazole systems, related to 2,3-disubstituted acrylonitriles as well as their cyclic analogues, benzimidazo[1,2-*a*]quinoline-6-carbonitriles exerted pronounced antiproliferative activity with *N*-methyl derivatives (**I** and **II**) showing selectivity in HeLa cells (IC_{50} = 0.8 and 0.7 μM, respectively) confirming a strong influence of the cyano group on improving the corresponding antiproliferative activity (Fig 1.) [11]. Several other studies confirmed the positive influence of the cyano group on biological activity [12].
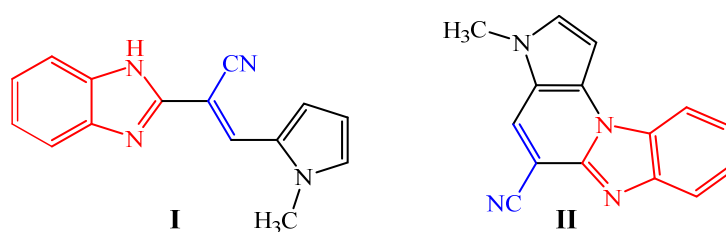

Figure 1. Previously published biologically active benzimidazolyl substuituted acrylonitriles.

This fact can be explained by a high level of polarity and electron-withdrawing properties, with substantially smaller volume and sterical requirements of the cyano group in comparison to, for example, the methyl group. Mentioned characteristics allow the cyano group the formation of hydrogen bonds essential for the binding to the key amino acid residues in the active site of various enzymes [13]. The introduction of the cyano group may also lead to the improvement of the physical and chemical properties, interaction with biological targets and enhanced molecule stability by hindering the *cis-trans* isomerism [14].

Furthermore, acrylonitriles bearing heteroaromatic or aromatic moieties have been recognized as promising biologically active compounds possessing a wide range of biological activities like anticancer [15,16], antituberculostatic [17], antibacterial [18,19] or antioxidative effects [20]. The synthesis and evaluation of antiproliferative activity of versatile acrylonitriles bearing benzotriazole or triazolo[4,5-*b/c*]pyridine nuclei has been described [21–23], where one of the studied compounds displaced radio labelled colchicine from its tubulin binding site with even lower IC_{50} value than colchicine itself (0.85 μM and 1.02 μM, respectively), thus confirming the high tubulin binding activity of these acrylonitrile derivatives. Fluorescence-based assays of the most active triazolo[4,5-*b/c*]pyridine substituted acrylonitriles (Fig. 2) also proved that these derivatives could interfere with the tubulin polymerization ($EC_{50(HeLa)}$ 0.65 μM) [24] as a mechanism of their antiproliferative activity.
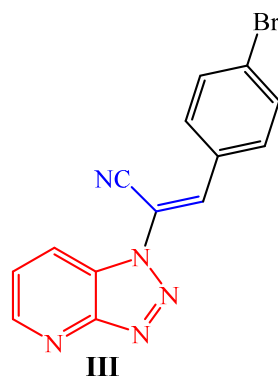

Figure 2. Triazolo[4,5-*b/c*]pyridine substituted acrylonitrile with a high tubulin affinity.

Based on these findings and together with the confirmed strong and promising antiproliferative potency of acrylonitrile derivatives, we designed novel *N*-substituted-2-benzimidazolyl acrylonitriles. Within the molecular hybridization of the mentioned pharmacophoric moieties, we have synthesized novel acrylonitrile derivatives and evaluated their antiproliferative activity towards eight human cancer and one non-cancerous cell lines.

To additionally explain the mechanism of the biological action of the most active and promising antiproliferative agents, their toxicity as well as the inhibition of the tubulin polymerization was studied. Lastly, to rationalize the antitumor activity of the most active compounds, the computational analysis of the binding within the colchicine binding site in tubulin was studied.

2. Results and Discussion

2.1. Chemistry

All newly designed acrylonitrile derivatives **28-43** were synthesized following the experimental procedure presented in Scheme 1.
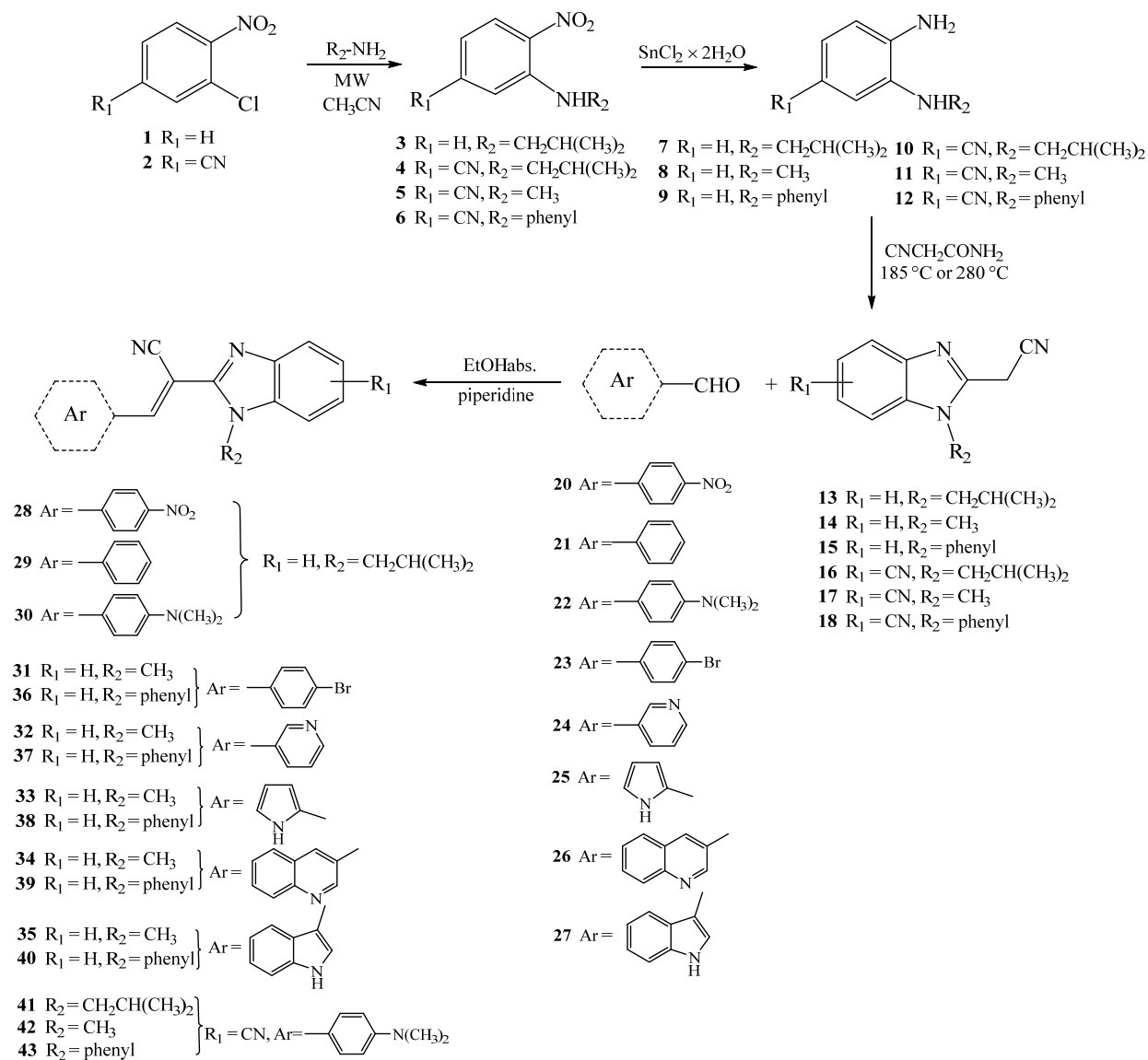
Scheme 1. The synthesis on *N*-substituted-2-benzimidazolyl acrylonitrile derivatives **28-42**.

As a main precursor for the synthesis of targeted derivatives, unsubstituted and cyano substituted *N*-isobutyl- **7** and **10** , *N*-methyl- **11** and *N*-phenyl-1,2-phenylenediamines **12** were prepared by the uncatalyzed microwave assisted amination starting from the corresponding *o*-chloronitrobenzenes **1-2**, followed by the reduction of compounds **3-6** with $SnCl_2 \times 2H_2O$ in MeOH. *N*-Substituted-2-cyanomethylbenzimidazoles **13-18** were obtained in the cyclocondensation reaction with 2-cyanoacetamide at high temperatures in moderate yields. Finally, within the condensation reaction of systems **13-18** with chosen aromatic aldehydes **20-27** in absolute ethanol followed by the addition of a few drops of piperidine as a weak base, corresponding *N*-substituted-2-benzimidazolyl acrylonitriles **28-43** were obtained in moderate to high reaction yields. All acrylonitrile derivatives were obtained as an *E*-isomer with the exception of compounds **28**, **30** and **41** which were a mixture of *E*- and *Z*-isomer and could not be efficiently separated by column chromatography.

The structures of newly prepared acrylonitriles were determined by both ^{1}H and ^{13}C NMR spectroscopies and elemental analysis. NMR analysis was based on the chemical shifts in both spectra and values of H-H coupling constants in the ^{1}H spectra. Reduction of the nitro group into the amino moiety was monitored by the appearance of the signals related to amino protons in the range of 5.25–4.08 ppm in the ^{1}H NMR spectra. Also, the formation of the desired acrylonitrile derivatives was confirmed by the appearance of a singlet related to the proton of acrylonitrile group in the range from 8.49–8.04 ppm.

2.2. Biological evaluation

2.2.1. Antiproliferative activity *in vitro*

All newly prepared compounds were tested for their antiproliferative activity *in vitro* on eight human cancer cells (Capan-1 - pancreatic adenocarcinoma, HCT-116 - colorectal carcinoma, NCI-H460 - lung carcinoma, DND-41 - acute lymphoblastic leukemia, HL-60 - acute myeloid leukemia, K-562 - chronic myeloid leukemia, MM.1S - multiple myeloma and Z-138 - non-Hodgkin lymphoma) as well as on a non-cancerous cell line hTERT RPE-1 (retina) using staurosporine and docetaxel as reference compounds. The results are expressed as IC_{50} values (50% inhibitory concentrations) and are summarized in Table 1. The majority of the compounds exerted a moderate to strong antiproliferative activity on the cell lines tested.

Table 1. Antiproliferative activity *in vitro* of tested compounds **28-43**

Cpd	$IC_{50}/\mu M$ *Cell line*								
	hTERT RPE-1	Capan-1	HCT-116	NCI-H460	DND-41	HL-60	K-562	MM.1S	Z-138
28	53.8	30.3	50.4	14.8	54.6	33.4	>100	72.9	45.4
29	44.9	20.6	42.4	26.1	60.0	29.1	53.4	66.7	40.1
30	**4.3**	**0.3**	**0.6**	**0.4**	**0.2**	**0.3**	**2.1**	**1.5**	**0.4**
31	47.3	20.5	52.2	32.1	41.3	24.3	57.6	95.7	30.7
32	60.1	57.1	85.1	59.3	>100	58.6	>100	>100	>100
33	>100	84.4	>100	67.9	73.7	>100	>100	>100	>100
34	39.4	66.9	>100	22.4	49.9	33.0	>100	>100	45.0
35	27.3	13.3	29.0	12.1	14.9	13.5	37.0	71.0	9.9
36	22.8	12.9	16.0	12.0	12.3	8.6	39.3	35.7	11.0
37	54.4	44.0	50.6	45.6	60.5	31.3	>100	59.5	30.2
38	32.4	14.2	49.4	27.4	41.2	42.0	>100	>100	67.5
39	12.2	10.0	12.4	13.6	14.1	15.3	>100	62.4	12.6
40	12.9	5.1	7.1	5.3	10.1	6.7	13.6	24.8	12.1
41	**1.7**	**0.2**	**0.4**	**0.6**	**0.3**	**0.2**	**1.4**	**1.3**	**0.4**
42	80.9	55.9	68.5	>100	>100	68.1	>100	>100	96.5
43	27.8	3.1	26.8	45.7	55.8	10.9	>100	>100	17.4
Docetaxel	0.0553	0.0088	0.0017	0.0024	0.0125	0.0072	0.0152	0.0118	0.0142
Staurosporine	0.0055	0.0123	0.0281	0.0597	0.0160	0.0076	0.0768	0.0442	0.0067

Most of the investigated compounds did not show any significant selectivity towards the tested cancer cell lines. Some of the derivatives exhibited strong and selective antiproliferative activity in submicromolar range of IC_{50} concentrations, but were less active in comparison to the used standard drugs. However, all of the tested systems were significantly less toxic against non-cancerous cell in comparison to reference staurosporine and docetaxel.

The most promising antiproliferative activity was observed for the *N,N*-dimethylamino substituted acrylonitrile derivative bearing the isobutyl side chain on benzimidazole nuclei (**30**) and the *N,N*-dimethylamino substituted acrylonitrile derivative having both the isobutyl side chain and cyano substituent on the benzimidazole nucleus (**41**). Among other systems with moderate activities, *N,N*-dimethylamino substituted acrylonitrile derivative bearing the phenyl ring and cyano substituent on a benzimidazole nucleus **43** showed selective activity towards Capan-1 (IC_{50} 3.1 μM) cells in comparison to all other tested cancer cells. Compound **40** with *N*-phenyl-2-benzimidazolyl-acrylonitrile attached to the position 3 of the indole nucleus, also showed significant antiproliferative activity against several cancer cells with IC_{50} 5.1 − 8.7 μM. Also, *p*-bromophenyl substituted acrylonitrile **36** with a phenyl ring attached to the benzimidazole nucleus displayed the best activity against HL-60 cells (IC_{50} 8.6 μM). Obtained results also revealed that among all tested compounds bearing a methyl or a phenyl substituent on the benzimidazole nucleus (**31-40** and **42-43**), the compounds with an *N*-phenylbenzimidazole core showed slightly improved antiproliferative activity in comparison to *N*-methyl substituted analogues. Also, a cyano group placed at the benzimidazole nucleus (compounds **42** and **43**) did not significantly improve antiproliferative activity. According to the obtained results, it is obvious that the most significant and important influence on the improvement of the antiproliferative activity resulted from the introduction of the *N,N*-dimethylaminophenyl ring in the structure of the targeted molecules **30** and **41** together with the isobutyl side chain placed at the *N*-position of benzimidazole nuclei. These important observations will be further confirmed by the computational analysis presented later. Additionally, the most active compounds **30** and **41** were tested on normal cells (PBMCs) and the obtained results revealed that both compounds did not affect these cells (Table 2).

Table 2. Toxicity of compounds **30** and **41** on normal cells

Cpd	IC_{50} / μM *PBMC*		
	donor 1	donor 2	donor 3
30	98,8	>100	>100
41	76,0	>100	>100
Staurosporine	0.001	0.0002	0.003

2.2.2. *In vitro* inhibition of the tubulin polymerization

To obtain an insight into the molecular mechanism of action of prepared derivatives and to investigate whether their antiproliferative activities are related to an interaction with tubulin, the most promising compounds **30** and **41** were tested for their *in vitro* ability to interfere with the tubulin polymerization process. Therefore, human cervix carcinoma HEp-2 was treated with the selected compounds, after which they were permeabilized and their tubulin was stained using anti-alpha tubulin antibody (Fig. 3). It turned out that systems **30** and **41** cause disintegration of the microtubule network, comparable with the effect of microtubule destabilizing reference compound vincristine and in contrast to the observed condensation in microtubule bundles caused by microtubule stabilizing reference compound docetaxel.
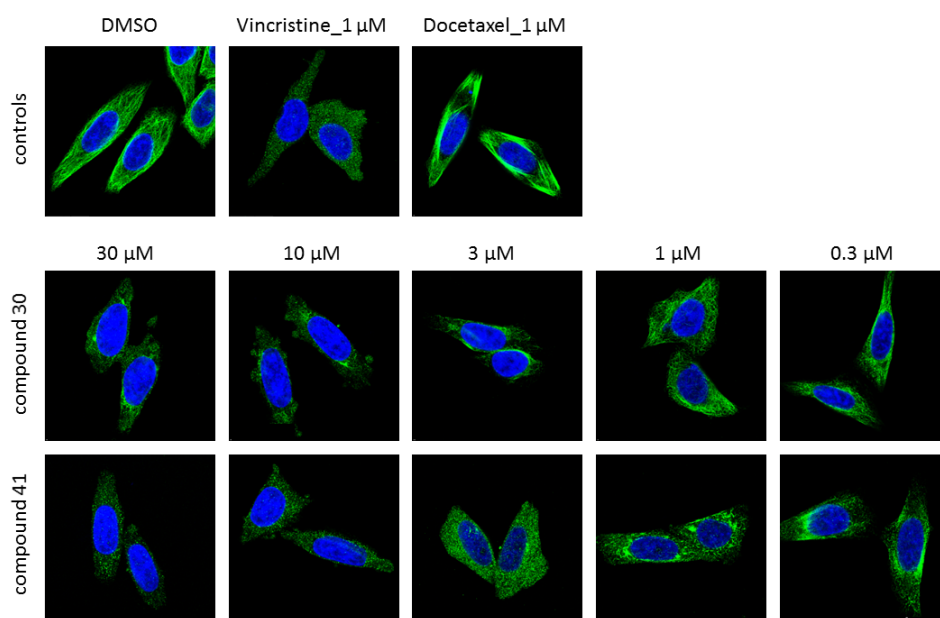

Figure 3. Immunofluorescence staining of alpha-tubulin in HEp-2 cells treated for 3 hours with indicated concentrations of compound **30** and **41**, or reference compounds vincristine and docetaxel. Green: alpha-tubulin, blue: DAPI. Scale bar: 20 μM

To provide a deeper and a more quantitative insight into the behavior of investigated systems, their potential interactions with tubulin were additionally followed by a variation of absorbance during the excitation at 350 nm and emission at 435 nm (Fig. 4) for 60 min using a standard tubulin polymerization assay, also employing docetaxel and vincristine as reference compounds and DMSO as a control. Both **30** and **41** were tested at a typical concentration of 30 μM, given that the literature advises it requires between 100 μM and 10 μM of the reference colchicine to achieve either full or 50% polymerization inhibition under equivalent conditions, respectively [25].
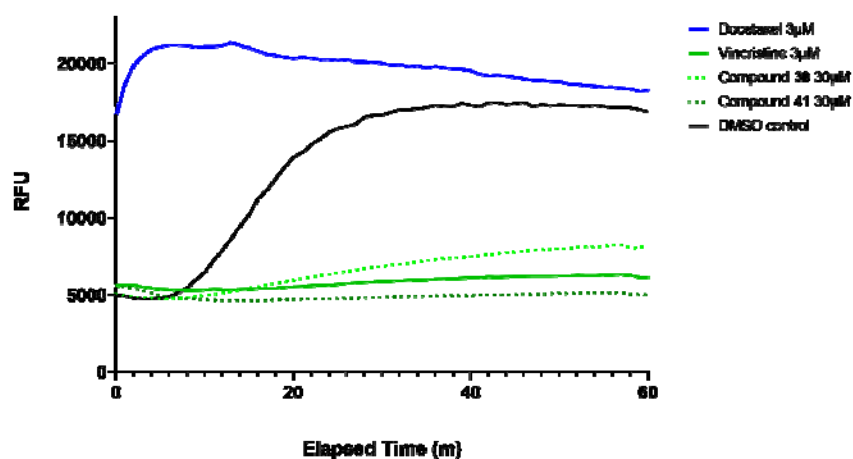
Figure 4. Effect of systems **30** and **41** on the *in vitro* tubulin polymerization. Purified porcine neuronal tubulin and GTP were mixed in a 96-well plate. Vincristine and docetaxel (3 μM) were used as reference systems, and DMSO as a vehicle control. The effect on tubulin assembly was recorder in a Tecan Spark multimode plate reader at 60 sec intervals for one hour at 37 °C. Each condition was tested in duplicate. Polymerization was measured by monitoring the excitation at 350 nm and emission at 435 nm.

Still, we note that the employed concentration required to inhibit tubulin polymerization is much higher than those required for the cytotoxicity, a phenomenon however well documented in the literature (see, for instance [26,27]). The *in vitro* experiments carried out with the investigated derivatives show different behaviors; the inhibition with **30** is highest at the beginning and it slowly declines over the course of the experiments, while an analogous effect of **41** is such that it quickly increases from the initial value to remain practically constant during the entire 60 minutes. Nevertheless, Figure 4 points to an important conclusion that both **30** and **41** show the inhibitory effect similar to that of vincristine, with **41** even surpassing the inhibitory potency of the reference system under these conditions. With this in mind, the latter led us to assume that molecular interactions that **30** and **41** form with tubulin are likely identical to those observed for vincristine, in line with other reports in the literature [24,25,28–30]. To further evaluate whether our compounds bind to the colchicine binding site of tubulin, N,N'-ethylene-bis(iodoacetamide) (EBI) competition assay was carried out in line with literature recommendations.[29–31] Although we have tried both Simple Western analysis and classical Western blot analysis for β-tubulin, and also using several different cell lines, in our hands the assay failed to perform as expected, likely due to differences in the optimal concentration and duration of the incubation of the tested systems [31] that would

require elaborate experimental optimization beyond the current scope. Nevertheless, based on the reported observations, particularly regarding the discussed similarity between our compounds and vincristine, we proceeded by performing molecular docking studies involving the examined lead compounds **30** and **41**, and inspecting different potential binding poses of both systems, yet focusing our attention on the main colchicine binding site located at the interface between the α- and β-tubulin subunits, taking colchicine as a control compound.

2.3. Computational analysis

Computational analysis was performed to offer more insight into the binding of the tested systems **30** and **41** on tubulin and interpret their experimentally observed activities towards microtubule formation. For that purpose, we employed docking simulations and quantum-chemical calculations with the aim of obtaining the binding poses and the accompanying binding energies, as well as providing features related to the electronic structure of these ligands. The analysis was also utilized on related **29** and **42**, with the idea of allowing enough structural and electronic information to offer some general conclusions about the studied compounds to aid in the design of even more potent ligands based on the employed organic framework. Given that microtubule-destabilizing agents typically bind either (i) to the vinca alkaloid site between two longitudinally aligned tubulin dimers (e.g. vinblastine), or (ii) to the colchicine site that is located at the intrasubunit interface within a tubulin dimer (e.g. colchicine) [32], we decided to also include colchicine (Fig. 5) in the analysis that will serve as a reference system, prompted by a better structural similarity with our ligands.
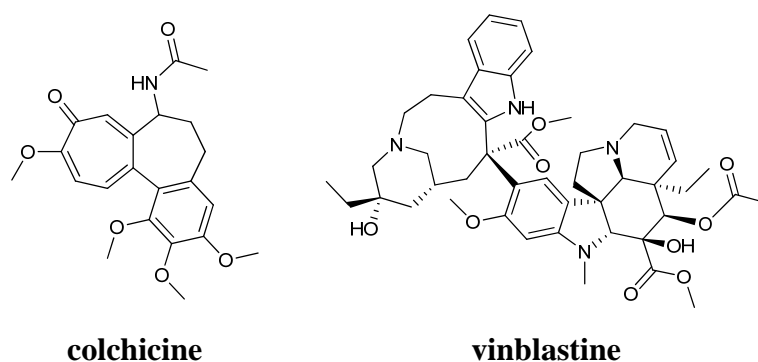

colchicine   **vinblastine**

Figure 5. Chemical structure of typical microtubule-destabilizing agents colchicine and vinblastine.

The calculated binding Gibbs free energies for all studied ligands are given in Table 3. It turns out that the highest affinity is predicted for colchicine, where it assumes ΔG_{bind} = −9.3 kcal mol^{-1}, placing our result in accordance with the binding energy reported by Silva-García and co-workers using the AutoDock docking software of ΔG_{bind} = −9.0 kcal mol^{-1} [25]. More importantly, both of these values are found in excellent agreement with the experimental value of $\Delta G_{bind,EXP}$ = −8.3 kcal mol^{-1} calculated from the measured colchicine binding constant $K_{bind,EXP}$ = 6.3 × 10^5 L mol^{-1} reported by Wilson and Meza [33]. In addition, the predicted binding position of colchicine very closely matches that of the crystal structure (Fig. 6), suggesting that docking procedure correctly positioned it within the colchicine binding site (Fig. 57S). Given the agreement in both the binding energy and the position of the ligand, we can safely conclude that these arguments lend a firm credence to the employed computational methodology and render other results reliable as well.

Table 3. The calculated binding Gibbs free energies ($\Delta G_{bind,CALC}$) between studied ligands and tubulin (in kcal mol^{-1}). The experimental value for colchicine ($\Delta G_{bind,EXP}$) is taken from ref. 25.

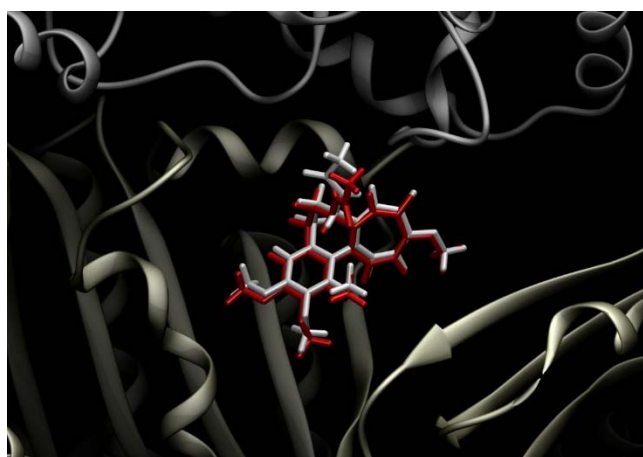|	**29**	**30**	**41**	**42**	**colchicine**
$\Delta G_{bind,CALC}$	−8.3	−8.6	−8.3	−8.1	−9.3
$\Delta G_{bind,EXP}$					−8.3

Figure 6. The overlap of colchicine structures as predicted through the docking procedure (in white) and that from the tubulin-colchicine crystal structure (in red), both positioned within the colchicine binding site between tubulin's subunits (α in grey and β in gold).

It appears that all four investigated ligands are weaker binders than colchicine (Table 3), being associated with between 0.7 (**30**) and 1.2 kcal mol^{-1} (**42**) less exergonic binding free energies. In addition, ligands employed here, namely **30** and **41**, surpass the affinity of the remaining two compounds, **29** and **42**, which justifies their experimental utilization against tubulin. Still, one notices identical binding affinities for **41** and **29**, yet with a distinct and significant difference. Although the employed docking procedure identified several binding positions for each ligand, a very important conclusion emerging from this analysis is that all compounds but **29** the most favourably bind within the colchicine binding site (Fig. 7), being the appropriate site for their activity. On the other hand, the binding affinity of $\Delta G_{bind} = -8.3$ kcal mol^{-1} for **29** relates to its position at the other end of the tubulin's β-subunit, which likely renders it different from other investigated ligands and interprets its lower antiproliferative activity. A closer analysis of the binding results shows that the most favourable position for **29** within the colchicine binding site is 0.5 kcal mol^{-1} less exergonic ($\Delta G_{bind} = -7.8$ kcal mol^{-1}), indicating that **29** has around 3 times lower affinity for that binding site, which is significant. The observed distinctions between **29** and, for example **30**, can be interpreted in the following way. These two systems differ in the presence of the *para*-NMe$_2$ group in **30**, which is absent in **29**. Given its strong electron-donating character, it is reasonable to expect that the effect of the attached NMe$_2$ group is channelized through its donation of the electronic density, primarily into the neighbouring phenyl moiety, and then to the rest of the system. This is evidenced in a significant reduction of the matching N–C bond distance from, for example, 1.460 Å in trimethylamine (NMe$_3$) to 1.368 Å calculated for **30**, being accompanied with a notable planarization of this group from 118.7° to 153.5° in the same order. A higher electron density in the mentioned phenyl group is significant for the binding. It appears that, within the binding site (Fig. 8), **30** is predominantly stabilized through cation⋯π interactions that its phenyl moiety bearing the NMe$_2$ group is making with the Lys352 residue, which clearly benefit from the increased electron density in the former aromatic framework. This interaction is further prompted by a likely N–H⋯N hydrogen bonding that Lys352 can make with the NMe$_2$ group in **30**. This helps explain why **30**, and other systems bearing the same NMe$_2$ functionality, namely **41** and **42**, show higher binding affinities than **29**, suggesting the necessity of such an electron-donating element within the structure to promote the binding.
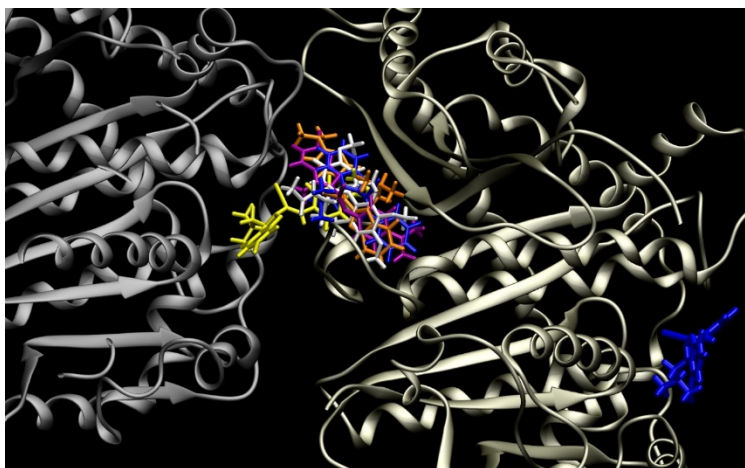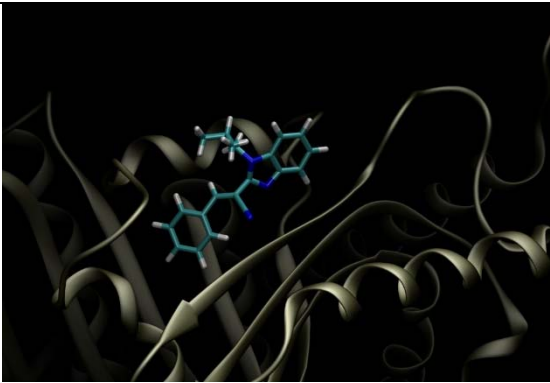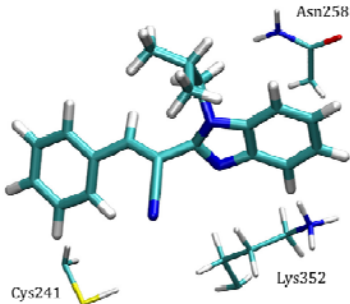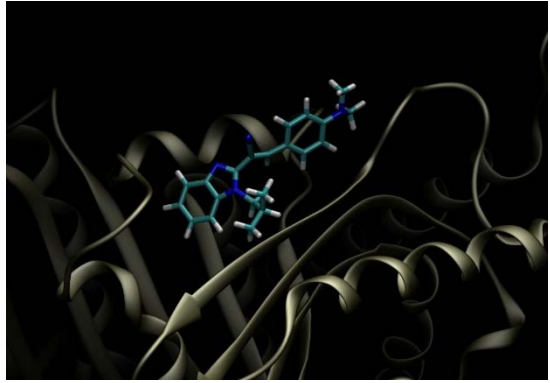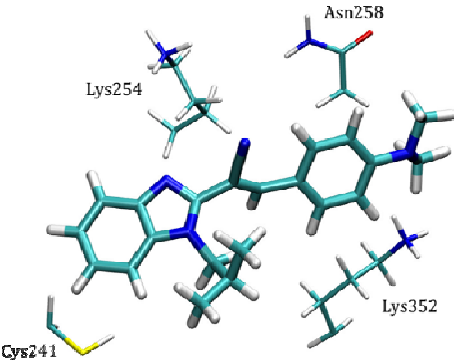
Figure 7. The most favourable binding position for investigated ligands. Colchicine is given in white, while other ligands are coloured blue (**29**), orange (**30**), yellow (**41**), and purple (**42**). Tubulin's subunits are given in grey (α) and gold (β).

In addition, the lack of this structural element in **29** results in its different binding pose (Fig. 8), which is rotated to position the benzimidazole unit in the favourable cation···π interactions with Lys352, while the unsubstituted phenyl group benefits from the hydrophobic interactions with Leu255, Leu242, Ile318 and Leu248, in this way orienting the –CN group for a likely C=N···H–S hydrogen bonding with Cys241. In **30**, the mentioned hydrophobic pocket is occupied by its benzimidazole fragment, allowing the –CN group to engage in hydrogen bonding with Lys254 and Asn258. In addition, Cys241 is located in the vicinity of **30** for the potential interactions either through S–H···N hydrogen bonds or S–H···π interactions with the benzimidazole unit. Given its different binding pose, all of these are missing in **29**, which make it a poorer binder. System **41** features the cyano group on the benzimidazole core, which makes it a 0.3 kcal mol^{-1} weaker binder than **30**. Unlike NMe$_2$, the cyano group is a strong electron-accepting moiety, clearly evidenced in the matching C(cyano)–C(phenyl) bond of 1.435 Å in **41**, being notably shorter than the value of 1.457 Å calculated for acetonitrile. As such, the cyano group depletes the electron density from the benzimidazole core, thus reducing its potential for the mentioned pairing with the Cys241, the latter only moderately compensated by some positive N–H···N≡C interactions of the introduced cyano group with Asn249. Moreover, this also modulates cation···π interactions with Lys352 observed in **30**, making Lys352 now more prone to interacting with the central cyano moiety through the N–H···N≡C hydrogen bonding, which is clearly a weaker contribution than the former. Lys254 again forms N–H···π contacts and hydrogen bonding with benzimidazole, the latter now occurring with the amino nitrogen bearing the isobutyl group (Fig. 8). This also results in a somewhat different orientation of **41**, where the large isobutyl moiety looks towards the tubulin's α-subunit, unlike in

30, where it points towards the β-subunit. The mentioned differences in the position and orientation of the *N*-isobutyl unit prompted us to inspect its effect on the overall binding, leading us to also consider system **42** being analogous to **41**, but with a smaller *N*-methyl unit. Its binding free energy is further reduced by 0.2 kcal mol^{-1} suggesting some significance for the affinity. Indeed, Fig. 8 reveals that this subtle modification gives considerable differences in the binding pose, as it allows an electron-deficient benzimidazole unit with the –CN group to benefit from the interaction with Lys352. Yet, these are obviously not as prominent as when the electron-enriched phenyl unit takes this role in **30** and **41**, thus offering the most dominant reason for the reduced affinity of **42**. The latter is somewhat compensated by a favourable S–H⋯N hydrogen bonding with the –NMe$_2$ group, still the overall binding free energy is the lowest among the three ligands. The introduced *N*-methyl group points towards the α-subunit and is too small to benefit from any hydrophobic interactions, unlike a larger *N*-isobutyl moiety which enjoys a range of interactions within the hydrophobic pocket, consisting mostly of Leu248, Ala354, Ile318 and Ala316 residues, as observed in **30**.

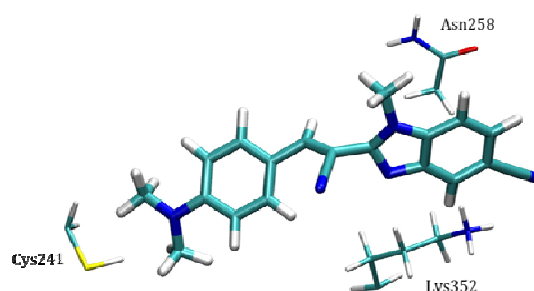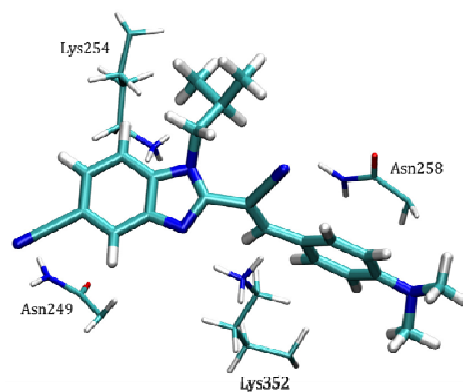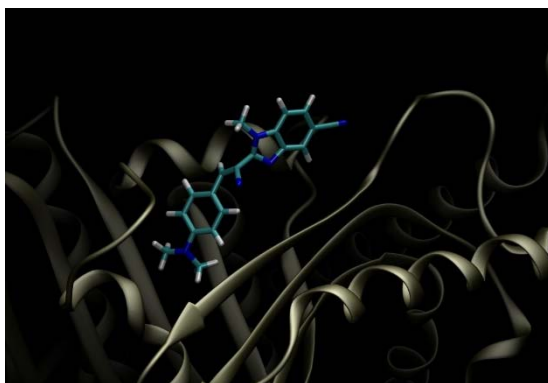| System	Binding position	Residues Affecting the Binding
29		
30		
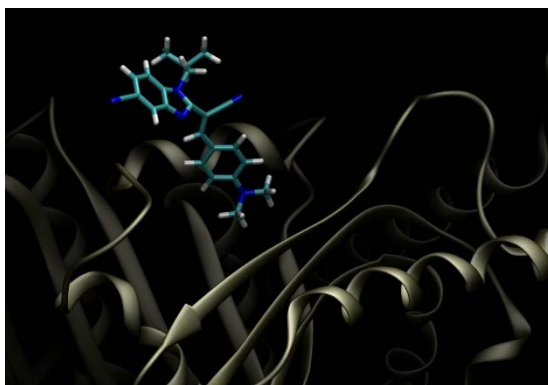
Figure 8. Binding of investigated ligands on the β-subunit of tubulin (left) and the identification of dominant residues governing the binding (right).

Lastly, let us comment on potential differences and the influence of different isomers on the observed affinities, focusing in particular on *E*- and *Z*-isomerism around the central C=C double bond, taking the most potent system **30** as an illustrative example. We find this necessary given that synthetic procedures employed here provided compound **30** as mixture of both isomers with a 5:1 ratio in favour of the E-analogue, as described in the Experimental part section later. Our DFT calculations at the (SMD)/M06–2X/6–31+G(d) level of theory confirm the higher stability of the *E*-isomer in **30**, being 1.3 kcal mol^{-1} more stable than its *Z*-analogue (Fig. 9). Even more so, the obtained difference in the stability translates to a 10:1 ratio in favour of the E-isomer, which, given a close agreement with the experimentally observed distribution, led us to primarily consider *E*-isomers in all four examined ligands, and these results were reported heretofore. This is further prompted by the calculated transition state structure connecting both isomers in **30** (ν_{imag} = 261i cm^{-1}), which was found 36.4 kcal mol^{-1} above the Gibbs free energy of the most stable *E*-isomer. The latter activation energy is clearly too high to allow for any conversion among isomers in solution, thus justifying the employed computational strategy, since it is reasonable to expect that analogous data for other compounds will be very similar.
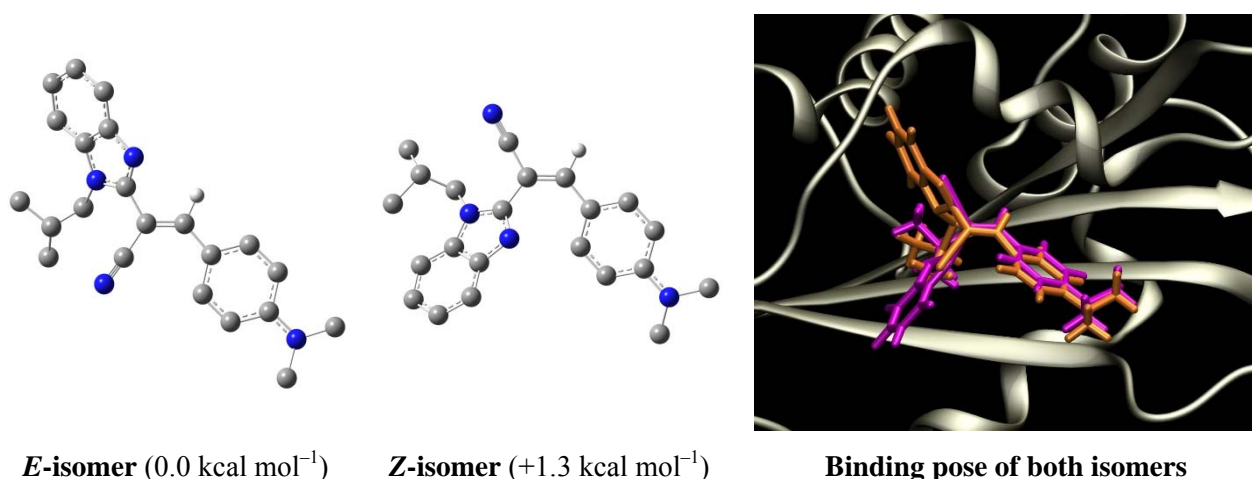
_E_-isomer (0.0 kcal mol^{-1})   **_Z_-isomer** (+1.3 kcal mol^{-1})   **Binding pose of both isomers**

Figure 9. The structure of the most stable _E_- (left) and _Z_-isomers (middle) of **30** and their relative stability calculated at the (SMD)/M06–2X/6–31+G(d) level of theory. All hydrogen atoms except the one within the central C=C double bond are omitted due to clarity. The most favourable binding poses for both isomers reveals binding within the same colchicine binding site in tubulin and a significant overlap of their phenyl–NMe$_2$ units (right, _E_-isomer in orange, _Z_-isomer in magenta).

Nevertheless, if both _E_- and _Z_-isomers in **30** are submitted to the docking calculations, it turns out that, just like its more stable analogue, the less stable _Z_-isomer is also most favourably positioned within the colchicine binding site (Fig. 9), yet with a slightly lower binding energy of $\Delta G_{\text{bind}} = -8.5$ kcal mol^{-1}. Given its lower affinity and its lower stability in solution, also acknowledging the high intrinsic barrier for the conversion among isomers, we can safely conclude that these results underline _E_-isomers as the likely active compounds in the performed experiments. Still, interestingly, the binding pose of both variants is such that it reveals a significant overlap in the dimethylamino-bound phenyl fragment, thus once again confirming the predominant importance of this structural element for the successful binding of the designed derivatives.

3. Conclusion

Here we present the design, synthesis and biological evaluation of novel 2-benzimidazolyl substituted acrylonitriles obtained in the cyclocondensation of the corresponding 2-cyanomethyl-benzimidazole with various aromatic aldehydes.

The benzimidazole nucleus was substituted on the *N*-position with either methyl, isobutyl or phenyl groups, with some derivatives also bearing a cyano group on the 5(6) position of benzimoidazole. All newly synthesized derivatives were tested on eight cancer cell lines and one non-cancerous cell. The majority of compounds displayed moderate antiproliferative activity without significant selectivity between tested cell lines. Most active and prominent derivatives were compounds **30** and **41** substituted with the *N,N*-dimethylaminophenyl ring bearing the isobutyl side chain placed at the *N*-position of the benzimidazole nucleus with and without the cyano substituent. These compounds showed nanomolar selective inhibitory activity (IC$_{50}$ 0.2 – 0.6 μM) against different cancer cell lines, while they did not affect normal cells (PBMCs). The obtained results suggest that there is a significant influence of the type of heteroaromatic ring attached to the acrylonitrile moiety as well as the type of the side chain placed at the *N*-position at the benzimidazole nuclei on the antiproliferative activity. Also, all of the tested compounds were less toxic towards non-cancerous cell and less active towards cancer cells in comparison to used standard drugs docetaxel and staurosporine. With this in mind, it remains a challenge to prove the low toxicity of the optimal derivatives at the level of animal experiments, but also to demonstrate acceptable pharmacokinetic properties and acceptable antitumor effect of the identified lead compounds *in vivo*, which is planned for the next phase of this research.

Further mechanistic studies demonstrated that this class of compounds inhibits cancer cell proliferation by disintegrating microtubules. This promotes systems **30** and **41** as lead compounds that will be further optimized in order to developed more efficient and even less toxic agents with significant antiproliferative activity (Fig. 10) and tubulin polymerization inhibition.

Computational analysis confirmed that the employed benzimidazole-acrylonitrile skeleton is structurally tuned to allow for the binding within the colchicine binding site in tubulin, with the affinity matching that of a colchicine itself, thus rationalizing its antitumor activity and justifying its application here. Still, small structural modifications of the parent core have a significant impact on both the binding position and the affinity of the prepared derivatives. The introduction of the electron-donating *para*-NMe$_2$ group on the phenyl unit turned out as the most dominant effect as it allows this part of the molecule to optimize its cation···π and hydrogen bonds with Lys352. Moreover, system **29** without the NMe$_2$ group comes with a reduced affinity and, even more importantly, is the most favourably positioned outside the colchicine binding site, thus further supporting the abovementioned conclusion. Addition of the electron-withdrawing cyano moiety on the benzimidazole core appears unfavourable as it reduces the ability of this part to engage in a favourable pairing with Cys241 and changes the binding pose to compensate that by some positive N–H···N≡C interactions of the introduced cyano group with Asn249. Both the mentioned cation···π

ability of Lys352 and the hydrogen-bonding tendency of Asn249 were already identified as crucial for the binding within the colchicine binding site [29,30], thus placing our results in firm agreement with earlier literature reports.

Lastly, computations clearly identified the necessity for a larger *N*-isobutyl unit, which directs the orientation of the ligand in such a way to allow the positioning of the former towards the tubulin's β-subunit and within its hydrophobic pocket consisting of Leu248, Ala354, Ile318 and Ala316 residues. Alternatively, smaller *N*-methyl substituent changes the orientation of the ligand so that the N–Me group points towards the α-subunit and engages in no particular favourable interactions on its own. When combined, these effects help in rationalizing the highest activity of **30** and **41** observed here.
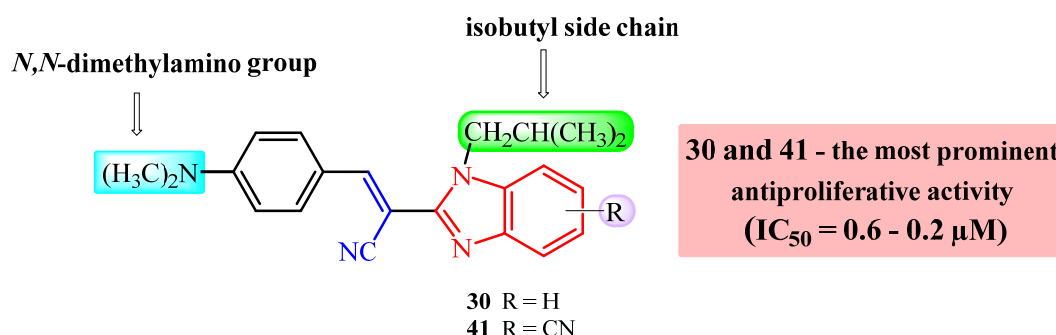
Figure 10. Systems **30** and **41** chosen for further optimization as promising agents with the antiproliferative activity

4. Experimental part

4.1. Chemistry

4.1.1. General methods

All chemicals and solvents were purchased from commercial suppliers Aldrich and Acros. Melting points were recorded on SMP11 Bibby and Büchi 535 apparatus. All NMR spectra were measured in DMSO-d_6 solutions using TMS as an internal standard. The ^{1}H and ^{13}C NMR spectra were recorded on a Varian Bruker Avance III HD 400 MHz/54 mm Ascend. Chemical shifts are reported in ppm (δ) relative to TMS. All compounds were routinely checked by TLC with Merck silica gel 60F-254 glass plates. Microwave-assisted synthesis was performed in a Milestone start S microwave oven using quartz cuvettes under the pressure of 40 bar. Elemental analysis for C, H and N were performed on a Perkin-Elmer 2400 elemental analyzer. Where analyses are indicated only as symbols of elements, analytical results obtained are within 0.4% of the theoretical value.

4.1.2. General method for preparation of compounds 3–6

Compounds **3–6** were prepared using microwave irradiation, at optimized reaction time at 170 °C with power 800 W and 40 bar pressure, from **1** or **2** in acetonitrile (10 mL) with excess of added corresponding amine. After cooling, resulting product was purified by column chromatography on SiO$_2$ using dichlormethane/methanol as eluent.

N-isobutyl-2-nitroaniline 3

3 was prepared from **1** (0.50 g, 3.2 mmol) and isobutylamine (3.15 mL, 31.8 mmol) after 3 h of irradiation to yield 0.64 g (86%) of orange oil. ^{1}H NMR (DMSO-d_6, 300 MHz): δ/ppm = 8.19 (bs, 1H, NH), 8.07 (dd, 1H, J_1 = 1.56 Hz, J_2 = 8.61 Hz, H$_{arom}$), 7.53 (td, 1H, J_1 = 1.25 Hz, J_2 = 8.42 Hz, H$_{arom}$), 7.06 (d, 1H, J = 8.46 Hz, H$_{arom}$), 6.68 (td, 1H, J_1 = 1.17 Hz, J_2 = 7.74 Hz, H$_{arom}$), 3.19 (t, 2H, J = 6.32 Hz, CH$_2$), 2.05–1.85 (m, 1H, CH), 0.96 (d, 6H, J = 6.66 Hz, CH$_3$); ^{13}C NMR (DMSO-d_6, 151 MHz): δ/ppm = 145.4, 136.6, 130.8, 126.2, 115.1, 114.6, 49.5, 27.2, 19.9 (2C); Anal. Calcd. for C$_{10}$H$_{14}$N$_2$O$_2$: C, 61.84; H, 7.27; N, 14.42. Found: C, 61.64; H, 7.35; N, 14.20%.

3-N-(isobutylamino)-4-nitrobenzonitrile 4

4 was prepared from **2** (0.50 g, 2.7 mmol) and isobutylamine (1.90 mL, 19.2 mmol) after 2 h of irradiation to yield 0.53 g (88%) of yellow powder. m.p. 99–101 °C; ^{1}H NMR (DMSO-d_6, 300 MHz): δ/ppm = 8.62 (t, 1H, J = 5.54 Hz, NH), 8.51 (d, 1H, J = 2.01 Hz, H$_{arom}$), 7.81 (dd, 1H, J_1 = 1.80 Hz, J_2 = 9.03 Hz, H$_{arom}$), 7.21 (d, 1H, J = 9.18 Hz, H$_{arom}$), 3.27 (t, 2H, J = 6.50 Hz, CH$_2$), 2.03–1.88 (m, 1H, CH), 0.95 (d, 6H, J = 6.66 Hz, CH$_3$); ^{13}C NMR (DMSO-d_6, 151 MHz): δ/ppm = 147.0, 137.5, 131.9, 130.7, 118.2, 115.9, 96.2, 49.5, 27.2, 19.8 (2C); Anal. Calcd. for C$_{11}$H$_{13}$N$_3$O$_2$: C, 60.26; H, 5.98; N, 19.17. Found: C, 60.39; H, 5.80; N, 19.30%.

3-N-(methylamino)-4-nitrobenzonitrile 5

5 was prepared from **2** (0.50 g, 2.7 mmol) and methylamine (2.60 mL, 58.3 mmol) after 2 h of irradiation to yield 0.46 g (94%) of yellow powder. m.p. 173–179 °C; ^{1}H NMR (DMSO-d_6, 300 MHz): δ/ppm = 8.64 (q, 1H, J = 5.50 Hz, NH), 8.49 (d, 1H, J = 2.01 Hz, H$_{arom}$), 7.84 (dd, 1H, J_1 = 1.64 Hz, J_2 = 9.08 Hz, H$_{arom}$), 7.10 (d, 1H, J = 9.12 Hz, H$_{arom}$), 3.00 (d, 3H, J = 4.98 Hz, CH$_3$); ^{13}C NMR (DMSO-d_6, 75 MHz): δ/ppm = 148.0, 138.1, 132.2, 131.2, 118.8, 116.1, 96.5, 30.4; Anal. Calcd. for C$_8$H$_7$N$_3$O$_2$: C, 54.24; H, 3.98; N, 23.72. Found: C, 54.04; H, 3.80; N, 23.95%.

4-nitro-3-N-(phenylamino)benzonitrile 6

6 was prepared from **2** (0.50 g, 2.7 mmol) and aniline (1.0 mL, 10.0 mmol) after 2 h of irradiation to yield 0.57 g (86%) of orange powder. m.p. 131–135 °C; ^{1}H NMR (DMSO-d_6, 300 MHz): δ/ppm = 9.90 (s, 1H, NH), 8.59 (d, 1H, J = 1.98 Hz, H$_{arom}$), 7.77 (dd, 1H, J_1 = 1.88 Hz, J_2 = 8.99 Hz, H$_{arom}$), 7.51–7.46 (m, 2H, H$_{arom}$), 7.37–7.30 (m, 3H, H$_{arom}$), 7.09 (d, 1H, J = 9.03 Hz, H$_{arom}$); ^{13}C NMR

(DMSO-d_6, 75 MHz): δ/ppm = 145.6, 138.3, 138.0, 132.9, 132.3, 130.2, 127.0, 126.0, 118.4, 117.7, 99.0; Anal. Calcd. for $C_{13}H_9N_3O_2$: C, 65.27; H, 3.79; N, 17.56. Found: C, 65.39; H, 3.99; N, 17.30%.

N-isobutylbenzene-1,2-diamine 7

3.20 g (16.5 mmol) of *N*-isobutyl-2-nitroaniline **3** and a solution of 22.30 g (98.8 mmol) $SnCl_2 \times 2H_2O$ in methanol (43 mL) and concentrated HCl (43 mL) were heated under reflux for 0.5 hours. After cooling, the reaction mixture was evaporated under vacuum and dissolved in water (70 mL). The resulting solution was treated with 20% NaOH to pH = 14. The resulting precipitate was filtered off and the filtrate was extracted with ethyl acetate. The organic layer was dried over anhydrous $MgSO_4$ and concentrated at reduce pressure to give the product as brown oil (2.19 g, 81%). ^{1}H NMR (DMSO-d_6, 300 MHz): δ/ppm = 6.53 (dd, 1H, J_1 = 1.60 Hz, J_2 = 7.70 Hz, H_{arom}), 6.47 (dd, 1H, J_1 = 1.97 Hz, J_2 = 7.13 Hz, H_{arom}), 6.43–6.32 (m, 2H, H_{arom}), 4.48 (s, 2H, NH_2), 4.33 (bs, 1H, NH), 2.82 (t, 2H, J = 6.05 Hz, CH_2), 1.95–1.78 (m, 1H, CH), 0.95 (d, 6H, J = 6.63 Hz, CH_3); Anal. Calcd. for $C_{10}H_{16}N_2$: C, 73.13; H, 9.82; N, 17.06. Found: C, 73.25; H, 9.89; N, 16.86%.

4.1.3. General method for preparation of compounds 10–12

Benzonitrile derivatives **4–5** and a solution of $SnCl_2 \times 2H_2O$ in MeOH and concentrated HCl were refluxed for 0.5 hours. After cooling, the reaction mixture was evaporated under vacuum and dissolved in water (70 mL). The resulting solution was treated with 20% NaOH to pH = 14. The resulting precipitate was filtered off, washed with hot ethanol and filtered. The filtrate was evaporated at a reduced pressure, a small amount of water was added and the product was filtered.

4-amino-3-(isobutylamino)benzonitrile 10

10 was prepared from **4** (2.64 g, 12.0 mmol), $SnCl_2 \times 2H_2O$ (21.75 g, 96.4 mmol), $HCl_{conc.}$ (32 mL) and H_2O (32 mL) to obtain a white powder (1.81 g, 79%). m.p. 120–125 °C; ^{1}H NMR (DMSO-d_6, 300 MHz): δ/ppm = 6.89 (dd, 1H, J_1 = 1.90 Hz, J_2 = 8.20 Hz, H_{arom}), 6.76 (d, 1H, J = 1.95 Hz, H_{arom}), 6.43 (d, 1H, J = 8.25 Hz, H_{arom}), 5,44 (bs, 1H, NH), 5.03 (s, 2H, NH_2), 2.91 (t, 2H, J = 6.18 Hz, NH), 1.95–1.82 (m, 1H, CH), 0.94 (d, 6H, J = 6.63 Hz, CH_3); ^{13}C NMR (DMSO-d_6, 75 MHz): δ/ppm = 140.5, 135.5, 123.2, 121.6, 115.1, 108.8, 96.6, 51.0, 27.4, 20.9 (2C); Anal. Calcd. for $C_{11}H_{15}N_3$: C, 69.81; H, 7.99; N, 22.20. Found: C, 69.95; H, 7.80; N, 22.25%.

4-amino-3-(methylamino)benzonitrile 11

11 was prepared from **5** (3.19 g, 18.0 mmol), $SnCl_2 \times 2H_2O$ (33.70 g, 149.4 mmol), $HCl_{conc.}$ (49 mL) and H_2O (49 mL) to obtain a light orange powder (1.62 g, 61%). m.p. 149–151 °C; ^{1}H NMR (DMSO-d_6, 300 MHz): δ/ppm = 6.95 (dd, 1H, J_1 = 1.90 Hz, J_2 = 8.15 Hz, H_{arom}), 6.77 (d, 1H, J = 1.95 Hz, H_{arom}), 6.41 (d, 1H, J = 8.19 Hz, H_{arom}), 5.57 (q, 1H, J = 5.82 Hz, NH), 4.89 (s, 2H, NH_2),

2.77 (d, 3H, J = 4.83 Hz, CH$_3$); ^{13}C NMR (DMSO-d_6, 75 MHz): δ/ppm = 141.6, 135.6, 123.5, 121.6, 114.9, 108.5, 96.9, 30.0; Anal. Calcd. for C$_{18}$H$_9$N$_3$: C, 65.29; H, 6.16; N, 28.55. Found: C, 65.10; H, 6.06; N, 24.84%.

4-amino-3-(phenylamino)benzonitrile 12

12 was prepared from **6** (2.64 g, 12.0 mmol), SnCl$_2$×2H$_2$O (22.15 g, 98.2 mmol), HCl$_{conc.}$ (32 mL) and H$_2$O (32 mL) to obtain a light yellow powder (2.20 g, 89%). m.p. 150–153 °C; ^{1}H NMR (DMSO-d_6, 300 MHz): δ/ppm = 7.52 (s, 1H, NH), 7.29–7.24 (m, 2H, H$_{arom}$), 7.09 (d, 1H, J = 8.19 Hz, H$_{arom}$), 7.03 (d, 2H, J = 7.56 Hz, H$_{arom}$), 7.00 (d, 1H, J = 1.92 Hz, H$_{arom}$), 6.94–6.87 (m, 2H, H$_{arom}$), 5.25 (s, 2H, NH$_2$); ^{13}C NMR (DMSO-d_6, 75 MHz): δ/ppm = 142.9, 139.7, 134.7, 129.7, 121.6, 121.3, 120.6, 118.8, 117.2, 116.8, 102.5; Anal. Calcd. for C$_{13}$H$_{11}$N$_3$: C, 74.62; H, 5.30; N, 20.08. Found: C, 74.70; H, 5.45; N, 19.85%.

4.1.4. General method for preparation of compounds 13–15

A mixture of corresponding substituted 1,2-phenylenediamine **7–9** and 2-cyanoacetamide was heated in an oil bath for 35–50 min at 185 °C. After cooling, resulting product was purified by column chromatography on SiO$_2$ using dichloromethane/methanol as eluent.

2-cyanomethyl-N-isobutylbenzimidazole 13

13 was prepared from *N*-isobutyl-1,2-phenylenediamine **7** (2.19 g, 13.3 mmol) and 2-cyanoacetamide (2.23 g, 26.6 mmol) after 45 min of heating to yield 1.52 g (54%) of brown oil. ^{1}H NMR (DMSO-d_6, 300 MHz): δ/ppm = 7.64 (dd, 1H, J_1 = 1.64 Hz, J_2 = 6.95 Hz, H$_{arom}$), 7.59 (dd, 1H, J_1 = 1.50 Hz, J_2 = 7.02 Hz, H$_{arom}$), 7.29–7.18 (m, 2H, H$_{arom}$), 4.52 (s, 2H, CH$_2$), 4.04 (d, 2H, J = 7.71 Hz, CH$_2$), 2.22–2.07 (m, 1H, CH), 0.87 (d, 6H, J = 6.66 Hz, CH$_3$); ^{13}C NMR (DMSO-d_6, 75 MHz): δ/ppm = 145.9, 142.2, 136.1, 122.9, 122.3, 119.3, 116.9, 111.3, 50.6, 29.0, 20.0, 17.9 (2C); MS (ESI): m/z= 214,19 ([M+1]$^+$); Anal. Calcd. for C$_{13}$H$_{15}$N$_3$: C, 73.21; H, 7.09; N, 19.70. Found: C, 73.01; H, 7.20; N, 19.79%.

2-Cyanomethyl-N-methylbenzimidazole 14 [34]

14 was prepared from *N*-methyl-1,2-phenylenediamine **8** (1.00 mL, 8.80 mmol) and 2-cyanoacetamide (1.48 g, 17.60 mmol) after 35 min of heating to yield 0.90 g (60%) of brown powder. m.p. 138–141 °C; ^{1}H NMR (DMSO-d_6, 300 MHz): δ/ppm = ^{1}H NMR (DMSO-d_6, 300 MHz): δ/ppm = 7.63 (dd, 1H, J_1 = 1.23 Hz, J_2 = 7.14 Hz, H$_{arom}$), 7.55 (dd, 1H, J_1 = 1.04 Hz, J_2 = 7.10 Hz, H$_{arom}$), 7.27 (td, 1H, J_1 = 1.39 Hz, J_2 = 7.52 Hz, H$_{arom}$), 7.21 (td, 1H, J_1 = 1.38 Hz, J_2 = 7.45 Hz, H$_{arom}$), 4.53 (s, 2H, CH$_2$), 3.76 (s, 3H, CH$_3$); ^{13}C NMR (DMSO-d_6, 75 MHz): δ/ppm = 146.1, 142.2, 136.4, 122.9, 122.2, 119.3, 116.7, 110.6, 30.3, 17.8; Anal. Calcd. for C$_{10}$H$_9$N$_3$: C, 70.16; H, 5.30; N, 24.54. Found: C, 70.44; H, 5.54; N, 24.68%.

2-Cyanomethyl-N-phenylbenzimidazole 15

15 was prepared from *N*-phenyl-1,2-phenylenediamine **9** (4.20 g, 22.8 mmol) and 2-cyanoacetamide (4.79 g, 57.0 mmol) after 50 min of heating to yield 1.57 g (30%) of brown powder. m.p. 130–135 °C; ^{1}H NMR (DMSO-d_6, 600 MHz): δ/ppm = 7.76 (d, 1H, J = 7.62 Hz, H_{arom}), 7.68–7.66 (m, 2H, H_{arom}), 7.61 (d, 1H, J = 7.26 Hz, H_{arom}), 7.58 (d, 2H, J = 7.26 Hz, H_{arom}), 7.30 (td, 1H, J_1 = 1.04 Hz, J_2 = 7.44 Hz, H_{arom}), 7.27 (td, 1H, J_1 = 0.94 Hz, J_2 = 7.50 Hz, H_{arom}), 7.17 (d, 1H, J = 7.50 Hz, H_{arom}), 4.36 (s, 2H, CH_2); ^{13}C NMR (DMSO-d_6, 75 MHz): δ/ppm = 145.6, 142.2, 136.7, 134.9, 130.7 (2C), 129.7, 127.4 (2C), 123.9, 123.1, 119.7, 116.5, 110.7, 18.6; Anal. Calcd. for $C_{15}H_{11}N_3$: C, 77.23; H, 4.75; N, 18.01. Found: C, 77.35; H, 4.83; N, 17.82%.

4.1.5. General method for preparation of compounds 16–18

A mixture of substituted benzonitriles **10**–**12** and 2-cyanoacetamide was heated for 5–20 min at 280 °C. After cooling, resulting product was purified by column chromatography on SiO_2 using dichloromethane/methanol as eluent.

5-cyano-2-cyanomethyl-N-isobutylbenzimidazole 16

16 was prepared from 3-amino-4-*N*-isobutylaminobenzonitrile **10** (1.81 g, 9.6 mmol) and 2-cyanoacetamide (1.60 g, 19.1 mmol) after 20 min of heating to yield 0.14 g (6%) of brown powder. m.p. 159–162 °C; ^{1}H NMR (DMSO-d_6, 400 MHz): δ/ppm = 8.23 (d, 1H, J = 1.04 Hz, H_{arom}), 7.85 (d, 1H, J = 8.44 Hz, H_{arom}), 7.68 (dd, 1H, J_1 = 1.52 Hz, J_2 = 8.44 Hz, H_{arom}), 4.62 (s, 2H, CH_2), 4.10 (d, 2H, J = 7.76 Hz, CH_2), 2.20–2.07 (m, 1H, CH), 0.86 (d, 6H, J = 6.64 Hz, CH_3); ^{13}C NMR (DMSO-d_6, 101 MHz): δ/ppm = 149.3, 141.7, 139.1, 126.4, 124.5, 120.2, 116.5, 113.0, 104.7, 50.8, 29.0, 20.0 (2C), 18.2; Anal. Calcd. for $C_{14}H_{14}N_4$: C, 70.57; H, 5.92; N, 23.51. Found: C, 70.45; H, 5.74; N, 23.81%.

5-cyano-2-cyanomethyl-N-methylbenzimidazole 17

17 was prepared from 3-amino-4-*N*-methylaminobenzonitrile **11** (1.58 g, 10.7 mmol) and 2-cyanoacetamide (1.80 g, 21.4 mmol) after 10 min of heating to yield 1.23 g (58%) of green powder. m.p. 248–252 °C; ^{1}H NMR (DMSO-d_6, 400 MHz): δ/ppm = 8.22 (d, 1H, J = 0.88 Hz, H_{arom}), 7.78 (d, 1H, J = 8.32 Hz, H_{arom}), 7.69 (dd, 1H, J_1 = 1.44 Hz, J_2 = 8.44 Hz, H_{arom}), 4.61 (s, 2H, CH_2), 3.81 (s, 3H, CH_3); ^{13}C NMR (DMSO-d_6, 101 MHz): δ/ppm = 149.6, 141.7, 139.3, 126.3, 124.3, 120.3, 116.4, 112.3, 104.5, 30.7, 18.1; Anal. Calcd. for $C_{11}H_8N_4$: C, 67.34; H, 4.11; N, 28.55. Found: C, 67.52; H, 4.30; N, 28.18%.

5-cyano-2-cyanomethyl-N-phenylbenzimidazole 18

18 was prepared from 3-amino-4-*N*-phenylaminobenzonitrile **12** (2.20 g, 10.5 mmol) and 2-cyanoacetamide (1.77 g, 21.0 mmol) after 5 min of heating to yield 0.93 g (34%) of yellow powder.

m.p. 136–139 °C; ^{1}H NMR (DMSO-d_6, 400 MHz): δ/ppm = 8.37 (d, 1H, J = 0.92 Hz, H$_{arom}$), 7.72–7.61 (m, 6H, H$_{arom}$), 7.33 (dd, 1H, J_1 = 0.46 Hz, J_2 = 8.42 Hz, H$_{arom}$), 4.43 (s, 2H, CH$_2$); ^{13}C NMR (DMSO-d_6, 101 MHz): δ/ppm = 149.0, 141.8, 139.5, 134.0, 130.8 (2C), 130.3, 127.5 (2C), 127.5, 124.8, 120.0, 116.1, 112.3, 105.4, 18.9; Anal. Calcd. for C$_{16}$H$_{10}$N$_4$: C, 74.40; H, 3.90; N, 21.69. Found: C, 74.23; H, 3.78; N, 21.99%.

4.1.6. General method for preparation of compounds 28–43

Solution of equimolar amounts of 2-cyanomethylbenzimidazoles **13–18**, corresponding heteroaromatic aldehydes **20–27** and few drops of piperidine in absolute ethanol, were refluxed for 2–5 hours. The cooled reaction mixture was filtered and, if necessary, product was purified by column chromatography on SiO$_2$ using dichloromethane/methanol as eluent.

E(Z)-2-(N-isobutylbenzimidazol -2-yl)-3-(4-nitrophenyl)acrylonitrile 28

28 was prepared from **13** (0.15 g, 0.7 mmol) and **20** (0.11 g, 0.7 mmol) in absolute ethanol (4 mL) after refluxing for 2 hours to yield 0.11 g (47%) of red oil in the form of a mixture of *E*- and *Z*-isomers in the ratio **28a:28b** = 2:1; **28a:** ^{1}H NMR (DMSO-d_6, 400 MHz): δ/ppm = 8.49 (s, 1H, H$_{arom}$), 8.43 (d, 2H, J = 8.84 Hz, H$_{arom}$), 8.25 (d, 2H, J = 8.72 Hz, H$_{arom}$), 7.75–7.73 (m, 2H, H$_{arom}$), 7.41–7.23 (m, 2H, H$_{arom}$), 4.39 (d, 2H, J = 7.52 Hz, CH$_2$), 2.25–2.12 (m, 1H, CH), 0.85 (d, 6H, J = 6.68 Hz, CH$_3$); MS (ESI): m/z= 347.27 ([M+1]$^+$); **28b:** ^{1}H NMR (DMSO-d_6, 400 MHz): δ/ppm = 7.86 (d, 1H, J = 8.04 Hz, H$_{arom}$), 7.75–7.73 (m, 1H, H$_{arom}$), 7.46 (d, 1H, J = 8.00 Hz, H$_{arom}$), 7.41–7.23 (m, 2H, H$_{arom}$), 7.27–7.25 (m, 1H, H$_{arom}$), 7.10 (t, 1H, J = 8.18 Hz, H$_{arom}$), 6.75 (t, 1H, J = 7.86 Hz, H$_{arom}$), 6.67 (s, 1H, H$_{arom}$), 1.10 (d, 3H, J = 6.68 Hz, CH$_3$), 1.01 (d, 3H, J = 6.64 Hz, CH$_3$), 0.92 (d, 1H, J = 6.68 Hz, CH), 0.24 (d, 2H, J = 6.60 Hz, CH$_2$); MS (ESI): m/z= 347.27 ([M+1]$^+$); ^{13}C NMR (DMSO-d_6, 101 MHz): δ/ppm = 149.1, 149.0, 146.5, 142.2, 139.2, 136.9, 131.3 (2C), 124.6 (2C), 124.3, 123.4, 120.0, 116.5, 112.2, 104.8, 51.4, 29.8, 20.0 (2C); Anal. Calcd. for C$_{20}$H$_{138}$N$_4$O$_2$: C, 69.35; H, 5.24; N, 16.17. Found: C, 69.56; H, 5.05; N, 16.30%.

E-2-(N-isobutylbenzimidazol -2-yl)-3-phenylacrylonitrile 29

29 was prepared from **13** (0.15 g, 0.7 mmol) and **21** (0.08 g, 0.7 mmol) in absolute ethanol (4 mL) after refluxing for 2 hours to yield 0.15 g (70%) of orange oil. ^{1}H NMR (DMSO-d_6, 400 MHz): δ/ppm = 8.31 (s, 1H, H$_{arom}$), 8.08–8.02 (m, 2H, H$_{arom}$), 7.76–7.71 (m, 2H, H$_{arom}$), 7.64–7.58 (m, 3H, H$_{arom}$), 7.35 (td, 1H, J_1 = 1.21 Hz, J_2 = 7.60 Hz, H$_{arom}$), 7.30 (td, 1H, J_1 = 1.13 Hz, J_2 = 7.56 Hz, H$_{arom}$), 4.36 (d, 2H, J = 7.50 Hz, CH$_2$), 2.23–2.12 (m, 1H, CH), 0.84 (d, 6H, J = 6.73 Hz, CH$_3$); ^{13}C NMR (DMSO-d_6, 101 MHz): δ/ppm = 151.7, 147.2, 142.2, 136.8, 133.2, 132.5, 130.2 (2C), 129.7 (2C), 123.9, 123.2, 119.9, 117.2, 112.0, 100.9, 51.3, 29.7, 20.0 (2C); Anal. Calcd. for C$_{20}$H$_{19}$N$_3$: C, 79.70; H, 6.35; N, 13.94. Found: C, 79.90; H, 6.30; N, 13.80%.

E(Z)-2-(N-isobutylbenzimidazol -2-yl)-3-(4-N,N-dimethylaminophenyl)acrylonitrile 30

30 was prepared from **13** (0.15 g, 0.7 mmol) and **22** (0.10 g, 0.7 mmol) in absolute ethanol (4 mL) after refluxing for 2 hours to yield 0.21 g (88%) of orange oil in the form of a mixture of *E*- and *Z*- isomers in the ratio **30a:30b** = 5:1; **30a:** ^{1}H NMR (DMSO-d_6, 400 MHz): δ/ppm = 8.07 (s, 1H, H_{arom}), 7.97 (d, 2H, J = 9.08 Hz, H_{arom}), 7.68–7.63 (m, 2H, H_{arom}), 7.31–7.22 (m, 2H, H_{arom}), 6.86 (d, 2H, J = 9.12 Hz, H_{arom}), 4.32 (d, 2H, J = 7.48 Hz, CH_2), 3.08 (s, 6H, CH_3), 2.22–2.13 (m, 1H, CH), 0.83 (d, 6H, J = 6.64 Hz, CH_3); ^{13}C NMR (DMSO-d_6, 101 MHz): δ/ppm = 153.2, 151.5 (2C), 148.7, 142.4, 136.9, 132.7, 123.2, 122.8, 120.3, 119.3, 118.9, 112.1, 111.6, 91.4, 51.2, 29.6, 20.0 (2C); **33b:** ^{1}H NMR (DMSO-d_6, 400 MHz): δ/ppm = 7.85 (s, 1H, H_{arom}), 7.75–7.70 (m, 2H, H_{arom}), 7.35–7.30 (m, 2H, H_{arom}), 6.86 (d, 2H, J = 9.12 Hz, H_{arom}), 6.56 (d, 2H, J = 9.16 Hz, H_{arom}), 3.82 (d, 2H, J = 7.60 Hz, CH_2), 2.93 (s, 6H, CH_3), 2.12–2.04 (m, 1H, CH), 0.79 (d, 6H, J = 6.64 Hz, CH_3); ^{13}C NMR (DMSO-d_6, 101 MHz): δ/ppm = 152.7, 151.4 (2C), 146.2, 143.0, 135.4, 132.3, 123.8, 122.8, 120.2, 120.0, 111.9, 111.6, 93.4, 51.2, 29.1, 20.1 (2C); Anal. Calcd. for $C_{22}H_{24}N_4$: C, 76.71; H, 7.02; N, 16.27. Found: C, 76.50; H, 7.25; N, 16.25%.

(E)-3-(4-bromophenyl)-2-(N-methylbenzimidazol-2-yl)acrylonitrile 31

31 was prepared from **14** (0.10 g, 0.6 mmol) and **23** (0.11 g, 0.6 mmol) in absolute ethanol (4 mL) after refluxing for 2 hours to yield 0.09 g (45%) of yellow powder. m.p 137–141 °C; ^{1}H NMR (DMSO-d_6, 400 MHz): δ/ppm = 8.18 (s, 1H, H_{arom}), 7.99 (d, 2H, J = 8.52 Hz, H_{arom}), 7.84 (d, 2H, J = 8.44 Hz, H_{arom}), 7.72 (d, 1H, J = 7.96 Hz, H_{arom}), 7.67 (d, 1H, J = 8.12 Hz, H_{arom}), 7.37 (t, 1H, J = 7.58 Hz, H_{arom}), 7.31 (t, 1H, J = 7.56 Hz, H_{arom}), 4.02 (s, 3H, CH_3); ^{13}C NMR (DMSO-d_6, 101 MHz): δ/ppm = 149.3, 147.6, 142.3, 137.1, 132.7 (2C), 132.5, 132.0 (2C), 125.8, 124.0, 123.2, 119.8, 117.0, 111.4, 102.0, 32.2; Anal. Calcd. for $C_{17}H_{12}BrN_3$: C, 60.37; H, 3.58; N, 12.42. Found: C, 60.50; H, 3.47; N, 12.60%.

(E)-2-(N-methylbenzimidazol-2-yl)-3-(pyridin-3-yl)acrylonitrile 32

32 was prepared from **14** (0.06 g, 0.3 mmol) and **24** (0.04 g, 0.3 mmol) in absolute ethanol (4 mL) after refluxing for 2 hours to yield 0.07 g (74%) of yellow powder. m.p 122–125 °C; ^{1}H NMR (DMSO-d_6, 400 MHz): δ/ppm = 9.10 (d, 1H, J = 2.16 Hz, H_{arom}), 8.74 (dd, 1H, J_1 = 1.50 Hz, J_2 = 4.78 Hz, H_{arom}), 8.49 (dt, 1H, J_1 = 1.69 Hz, J_2 = 8.08 Hz, H_{arom}), 8.26 (s, 1H, H_{arom}), 7.73 (d, 1H, J = 7.88 Hz, H_{arom}), 7.70–7.64 (m, 2H, H_{arom}), 7.38 (td, 1H, J_1 = 1.08 Hz, J_2 = 7.61 Hz, H_{arom}), 7.31 (td, 1H, J_1 = 1.12 Hz, J_2 = 8.12 Hz, H_{arom}), 4.04 (s, 3H, CH_3); ^{13}C NMR (DMSO-d_6, 101 MHz): δ/ppm = 152.3, 151.5, 147.4, 147.3, 142.3, 137.1, 136.1, 129.5, 124.5, 124.1, 123.3, 119.9, 116.8, 111.4, 103.7, 32.2; Anal. Calcd. for $C_{16}H_{12}N_4$: C, 73.83; H, 4.65; N, 21.52. Found: C, 73.65; H, 4.50; N, 21.85%.

(E)-2-(N-methylbenzimidazol-2-yl)-3-(1H-pyrrol-2-yl)acrylonitrile 33

33 was prepared from **14** (0.10 g, 0.6 mmol) and **25** (0.05 g, 0.6 mmol) in absolute ethanol (4 mL) after refluxing for 2 hours to yield 0.10 g (65%) of brown powder. m.p. 185–189 °C; ^{1}H NMR (DMSO-d_6, 400 MHz): δ/ppm = 11.84 (s, 1H, NH), 8.13 (s, 1H, H_{arom}), 7.64 (dd, 1H, J_1 = 1.16 Hz, J_2 = 7.20 Hz, H_{arom}), 7.60 (dd, 1H, J_1 = 1.06 Hz, J_2 = 7.26 Hz, H_{arom}), 7.38 (bs, 1H, H_{arom}), 7.32 (bs, 1H, H_{arom}), 7.29 (td, 1H, J_1 = 1.38 Hz, J_2 = 7.82 Hz, H_{arom}), 7.25 (td, 1H, J_1 = 1.32 Hz, J_2 = 7.45 Hz, H_{arom}), 6.45 (bs, 1H, H_{arom}), 3.99 (s, 3H, CH$_3$); ^{13}C NMR (DMSO-d_6, 101 MHz): δ/ppm = 148.6, 142.5, 139.6, 137.2, 127.7, 126.0, 123.1, 122.8, 119.1, 118.6, 114.7, 112.7, 112.0, 90.3, 32.0; Anal. Calcd. for $C_{15}H_{12}N_4$: C, 72.56; H, 4.87; N, 22.57. Found: C, 72.40; H, 4.98; N, 22.62%.

(E)-2-(N-methylbenzimidazol-2-yl)-3-(quinolin-3-yl)acrylonitrile 34

34 was prepared from **14** (0.10 g, 0.6 mmol) and **26** (0.09 g, 0.6 mmol) in absolute ethanol (4 mL) after refluxing for 2 hours to yield 0.07 g (37%) of yellow powder. m.p. 165–170 °C; ^{1}H NMR (DMSO-d_6, 400 MHz): δ/ppm = 9.41 (d, 1H, J = 2.28 Hz, H_{arom}), 9.03 (d, 1H, J = 2.16 Hz, H_{arom}), 8.44 (s, 1H, H_{arom}), 8.16 –8.11 (m, 2H, H_{arom}), 7.93 (td, 1H, J_1 = 1.39 Hz, J_2 = 7.71 Hz, H_{arom}), 7.75 (d, 2H, J = 7.44 Hz, H_{arom}), 7.71 (d, 1H, J = 7.96 Hz, H_{arom}), 7.39 (td, 1H, J_1 = 1.13 Hz, J_2 = 7.61 Hz, H_{arom}), 7.33 (td, 1H, J_1 = 1.12 Hz, J_2 = 7.57 Hz, H_{arom}), 3.99 (s, 3H, CH$_3$); ^{13}C NMR (DMSO-d_6, 101 MHz): δ/ppm = 148.6, 142.5, 139.6, 137.2, 127.7, 126.0, 123.1, 122.8, 119.1, 118.6, 114.7, 112.7, 110.9, 90.3, 32.0; Anal. Calcd. for $C_{20}H_{14}N_4$: C, 77.40; H, 4.55; N, 18.05. Found: C, 77.21; H, 4.35; N, 18.44%.

(E)-3-(1H-indol-2-yl)-2-(N-methylbenzimidazol-2-yl)acrylonitrile 35

35 was prepared from **14** (0.10 g, 0.6 mmol) and **27** (0.08 g, 0.6 mmol) in absolute ethanol (4 mL) after refluxing for 3 hours to yield 0.16 g (94%) of light green powder. m.p. 239–242 °C; ^{1}H NMR (DMSO-d_6, 400 MHz): δ/ppm = 12.30 (s, 1H, NH), 8.55 (s, 1H, H_{arom}), 8.44 (s, 1H, H_{arom}), 8.00 (d, 1H, J = 7.56 Hz, H_{arom}), 7.69 (d, 1H, J = 7.36 Hz, H_{arom}), 7.63 (d, 1H, J = 7.56 Hz, H_{arom}), 7.58 (d, 1H, J = 7.80 Hz, H_{arom}), 7.34–7.29 (m, 2H, H_{arom}), 7.28–7.22 (m, 2H, H_{arom}), 4.02 (s, 3H, CH$_3$); ^{13}C NMR (DMSO-d_6, 101 MHz): δ/ppm = 148.9, 142.7, 142.5, 137.1, 136.4, 129.6, 127.6, 123.7, 123.1, 122.8, 121.9, 119.4, 119.3, 119.0, 113.1, 111.0, 92.0, 56,5, 32.0; Anal. Calcd. for $C_{19}H_{14}N_4$: C, 76.49; H, 4.73; N, 18.78. Found: C, 76.62; H, 4.60; N, 18.80%.

(E)-3-(4-bromophenyl)-2-(N-phenylbenzimidazol-2-yl)acrylonitrile 36

36 was prepared from **15** (0.13 g, 0.5 mmol) and **23** (0.19 g, 0.5 mmol) in absolute ethanol (4 mL) after refluxing for 2 hours to yield 0.15 g (70%) of yellow powder. m.p. 154–157 °C; ^{1}H NMR (DMSO-d_6, 300 MHz): δ/ppm = 7.92 (s, 1H, H_{arom}), 7.84 (dd, 1H, J_1 = 2.45 Hz, J_2 = 6.23 Hz, H_{arom}), 7.75 (s, 4H, H_{arom}), 7.70–7.58 (m, 5H, H_{arom}), 7.41–7.32 (m, 2H, H_{arom}), 7.23 (dd, 1H, J_1 = 2.46 Hz, J_2 = 6.36 Hz, H_{arom}); ^{13}C NMR (DMSO-d_6, 75 MHz): δ/ppm = 140.9, 133.7, 133.3, 132.2, 131.9,

131.1, 130.7, 129.0, 127.7, 127.4, 126.4, 124.7, 124.4, 123.9, 121.7, 119.9, 116.1, 115.5; Anal. Calcd. for $C_{22}H_{14}BrN_3$: C, 66.01; H, 3.53; N, 10.50. Found: C, 66.23; H, 3.68; N, 10.25%.

(E)-2-(N-phenylbenzimidazol-2-yl)-3-(pyridin-3-yl)acrylonitrile 37

37 was prepared from **15** (0.22 g, 0.9 mmol) and **24** (0.10 g, 0.9 mmol) in absolute ethanol (4 mL) after refluxing for 2 hours to yield 0.22 g (73%) of yellow powder. m.p. 164–168 °C; ^{1}H NMR (DMSO-d_6, 400 MHz): δ/ppm = 8.86 (d, 1H, J = 2.24 Hz, H_{arom}), 8.70 (dd, 1H, J_1 = 1.56 Hz, J_2 = 4.80 Hz, H_{arom}), 8.31 (dt, 1H, J_1 = 1.76 Hz, J_2 = 8.08 Hz, H_{arom}), 8.05 (s, 1H, H_{arom}), 7.85 (dd, 1H, J_1 = 1.84 Hz, J_2 = 6.76 Hz, H_{arom}), 7.70–7.63 (m, 5H, H_{arom}), 7.59 (dd, 1H, J_1 = 4.82 Hz, J_2 = 8.10 Hz, H_{arom}), 7.42–7.34 (m, 2H, H_{arom}), 7.25 (dd, 1H, J_1 = 1.86 Hz, J_2 = 6.86 Hz, H_{arom}); ^{13}C NMR (DMSO-d_6, 101 MHz): δ/ppm = 152.5, 151.3, 147.8, 146.6, 142.4, 137.4, 135.9, 135.5, 130.7 (2C), 130.1, 129.1, 128.0 (2C), 125.0, 124.6, 124.0, 120.2, 115.5, 111.2, 103.3; Anal. Calcd. for $C_{21}H_{14}N_4$: C, 78.24; H, 4.38; N, 17.38. Found: C, 78.04; H, 4.66; N, 17.30%.

(E)-2-(N-phenylbenzimidazol-2-yl)-3-(1H-pyrrol-2-yl)acrylonitrile 38

38 was prepared from **15** (0.24 g, 1.0 mmol) and **25** (0.10 g, 1.0 mmol) in absolute ethanol (4 mL) after refluxing for 2 hours to yield 0.25 g (78%) of light green powder. m.p. 181–186 °C; ^{1}H NMR (DMSO-d_6, 400 MHz): δ/ppm = 11.82 (s, 1H, NH), 8.06 (s, 1H, H_{arom}), 7.74 (d, 1H, J = 7.72 Hz, H_{arom}), 7.68–7.57 (m, 5H, H_{arom}), 7.32 (td, 1H, J_1 = 1.15 Hz, J_2 = 7.54 Hz, H_{arom}), 7.29–7.25 (m, 2H, H_{arom}), 7.21 (d, 1H, J = 3.72 Hz, H_{arom}), 7.14 (d, 1H, J = 7.72 Hz, H_{arom}), 6.38 (t, 1H, J = 2.96 Hz, H_{arom}); ^{13}C NMR (DMSO-d_6, 101 MHz): δ/ppm = 148.3, 142.5, 139.7, 137.5, 135.7, 130.5 (2C), 129.9, 128.1 (2C), 127.6, 126.1, 123.9, 123.5, 119.3, 117.1, 114.8, 112.7, 110.8, 90.3; Anal. Calcd. for $C_{20}H_{14}N_4$: C, 77.40; H, 4.55; N, 18.05. Found: C, 77.70; H, 4.62; N, 17.68%.

(E)-2-(N-phenylbenzimidazol-2-yl)-3-(quinolin-3-yl)acrylonitrile 39

39 was prepared from **15** (0.10 g, 0.4 mmol) and **26** (0.07 g, 0.4 mmol) in absolute ethanol (4 mL) after refluxing for 5 hours to yield 0.12 g (72%) of light yellow powder. m.p. 177–179 °C; ^{1}H NMR (DMSO-d_6, 400 MHz): δ/ppm = 9.18 (d, 1H, J = 2.28 Hz, H_{arom}), 8.87 (d, 1H, J = 2.00 Hz, H_{arom}), 8.23 (s, 1H, H_{arom}), 8.08 (d, 2H, J = 9.40 Hz, H_{arom}), 7.92–7.86 (m, 2H, H_{arom}), 7.73–7.63 (m, 6H, H_{arom}), 7.41 (td, 1H, J_1 = 1.37 Hz, J_2 = 7.11 Hz, H_{arom}), 7.37 (td, 1H, J_1 = 1.35 Hz, J_2 = 7.17 Hz, H_{arom}), 7.26 (dd, 1H, J_1 = 1.68 Hz, J_2 = 6.96 Hz, H_{arom}); ^{13}C NMR (DMSO-d_6, 101 MHz): δ/ppm = 150.8, 148.5, 147.7, 146.7, 142.4, 137.4, 137.2, 135.5, 132.4, 130.7 (2C), 130.1, 129.7, 129.3, 128.3, 128.0 (2C), 127.1, 126.5, 125.0, 124.1, 120.2, 115.7, 111.2, 103.1; Anal. Calcd. for $C_{25}H_{16}N_4$: C, 80.63; H, 4.33; N, 15.04. Found: C, 80.55; H, 4.21; N, 15.24%.

(E)-3-(1H-indol-3-yl)-2-(N-phenylbenzimidazol-2-yl)acrylonitrile 40

40 was prepared from **15** (0.16 g, 0.7 mmol) and **27** (0.10 g, 0.7 mmol) in absolute ethanol (4 mL) after refluxing for 5 hours to yield 0.20 g (82%) of light yellow powder. m.p. 238–242 °C; ^{1}H NMR

(DMSO-d_6, 400 MHz): δ/ppm = 12.26 (s, 1H, NH), 8.40 (s, 1H, H$_{arom}$), 7.95 (s, 1H, H$_{arom}$), 7.80 (d, 1H, J = 7.52 Hz, H$_{arom}$), 7.73–7.64 (m, 5H, H$_{arom}$), 7.53 (d, 1H, J = 8.08 Hz, H$_{arom}$) 7.37–7.30 (m, 2H, H$_{arom}$), 7.28 (td, 1H, J_1 = 1.24 Hz, J_2 = 7.28 Hz, H$_{arom}$), 7.24 (td, 1H, J_1 = 1.00 Hz, J_2 = 8.08 Hz, H$_{arom}$), 7.16 (t, 2H, J = 7.42 Hz, H$_{arom}$); ^{13}C NMR (DMSO-d_6, 101 MHz): δ/ppm = 148.2, 142.7, 141.5, 137.7, 136.3, 136.2, 130.8 (2C), 130.0, 129.4, 128.3 (2C), 127.4, 124.0, 123.7, 123.5, 121.9, 119.6, 118.4, 118.0, 113.2, 110.7, 110.4, 92.6; Anal. Calcd. for C$_{24}$H$_{16}$N$_4$: C, 79.98; H, 4.47; N, 15.55. Found: C, 79.80; H, 4.40; N, 15.80%.

E(Z)-2-(5-cyano-N-isobutylbenzimidazol-2-yl)-3-(4-N,N-dimethylaminophenyl)acrylonitrile 41

41 was prepared from **16** (0.10 g, 0.4 mmol) and **22** (0.06 g, 0.4 mmol) in absolute ethanol (2.5 mL) after refluxing for 1.5 hours to yield 0.01 g (8%) of orange oil in the form of a mixture of *E*- and *Z*-isomers in the ratio **41a:41b** = 3:1; **41a:** ^{1}H NMR (DMSO-d_6, 400 MHz): δ/ppm = 8.34 (d, 1H, J = 0.92 Hz, H$_{arom}$), 7.95 (d, 1H, J = 8.48 Hz, H$_{arom}$), 7.91 (s, 1H, H$_{arom}$), 7.77 (dd, 1H, J_1 = 1.52 Hz, J_2 = 8.48 Hz, H$_{arom}$), 6.86 (d, 2H, J = 9.24 Hz, H$_{arom}$), 6.58 (d, 2H, J = 9.20 Hz, H$_{arom}$), 3.88 (d, 2H, J = 7.60 Hz, CH$_2$), 2.94 (s, 6H, CH$_3$), 2.10–2.02 (m, 1H, CH), 0.78 (d, 6H, J = 6.64 Hz, CH$_3$); ^{13}C NMR (DMSO-d_6, 101 MHz): δ/ppm = 152.9, 152.2, 149.2, 142.4, 138.4, 132.5 (2C), 127.0, 125.3, 120.0, 119.7 (2C), 113.8, 112.0 (2C), 105.3, 92.0, 51.5, 39.9 (2C), 29.2, 20.0 (2C); MS (ESI): *m/z*= 370.37 ([M+1]$^+$); **41b:** ^{1}H NMR (DMSO-d_6, 400 MHz): δ/ppm = 8.24 (d, 1H, J = 1,00 Hz, H$_{arom}$), 8.17 (s, 1H, H$_{arom}$), 7.99 (d, 2H, J = 9.12 Hz, H$_{arom}$), 7.91 (d, 1H, J = 8.16 Hz, H$_{arom}$), 7.69 (dd, 1H, J_1 = 1.50 Hz, J_2 = 8.50 Hz, H$_{arom}$), 6.87 (d, 2H, J = 9.32 Hz, H$_{arom}$), 4.39 (d, 2H, J = 7.56 Hz, CH$_2$), 3.09 (s, 6H, CH$_3$), 2.19–2.13 (m, 1H, CH), 0.84 (d, 6H, J = 6.68 Hz, CH$_3$); ^{13}C NMR (DMSO-d_6, 101 MHz): δ/ppm = 153.5, 152.5, 151.5, 141.8, 139.9, 133.0 (2C), 126.4, 124.1, 120.2, 118.6 (2C), 113.2, 112.2 (2C), 105.0, 90.1, 51.4, 40.2 (2C), 29.7, 19.9 (2C); MS (ESI): *m/z*= 370.37 ([M+1]$^+$); Anal. Calcd. for C$_{23}$H$_{23}$N$_5$: C, 74.77; H, 6.27; N, 18.96. Found: C, 74.87; H, 6.38; N, 18.75%.

(E)-2-(5-cyano-N-methylbenzimidazol-2-yl)-3-(4-N,N-dimethylaminophenyl)acrylonitrile 42

42 was prepared from **17** (0.15 g, 0.7 mmol) and **22** (0.12 g, 0.7 mmol) in absolute ethanol (2.5 mL) after refluxing for 2 hours to yield 0.03 g (13%) of orange powder. m.p. 290–293 °C; ^{1}H NMR (DMSO-d_6, 400 MHz): δ/ppm = 8.20 (d, 1H, J = 0.72 Hz, H$_{arom}$), 8.04 (s, 1H, H$_{arom}$), 7.99 (d, 2H, J = 9.08 Hz, H$_{arom}$), 7.83 (d, 1H, J = 8.44 Hz, H$_{arom}$), 7.70 (dd, 1H, J_1 = 1.40 Hz, J_2 = 8.40 Hz, H$_{arom}$), 6.87 (d, 2H, J = 9.04 Hz, H$_{arom}$), 4.02 (s, 3H, CH$_3$), 3.09 (s, 6H, CH$_3$); ^{13}C NMR (DMSO-d_6, 101 MHz): δ/ppm = 153.4, 151.8, 141.9, 140.0, 133.1, 132.9, 126.4, 124.3, 124.0, 120.3, 120.1, 118.6, 112.6, 112.3, 112.1, 111.5, 104.9, 90.7, 40.6, 40.4, 32.5; MS (ESI): *m/z*= 328.32 ([M+1]$^+$); Anal. Calcd. for C$_{20}$H$_{17}$N$_5$: C, 73.37; H, 5.23; N, 21.39. Found: C, 73.17; H, 5.16; N, 21.67%.

(E)-2-(5-cyano-N-phenylbenzimidazol-2-yl)-3-(4-N,N-dimethylaminophenyl)acrylonitrile 43

43 was prepared from **18** (0.10 g, 0.4 mmol) and **22** (0.06 g, 0.4 mmol) in absolute ethanol (2.5 mL) after refluxing for 1.5 hours to yield 0.01 g (7%) of yellow powder. m.p. 242–248 °C; ^{1}H NMR (DMSO-d_6, 400 MHz): δ/ppm = 8.32 (d, 1H, J = 0.92 Hz, H$_{arom}$), 7.77 (s, 1H, H$_{arom}$), 7.73 (d, 2H, J = 9.12 Hz, H$_{arom}$), 7.70–7.61 (m, 6H, H$_{arom}$), 7.29 (dd, 1H, J_1 = 0.38 Hz, J_2 = 8.42 Hz, H$_{arom}$), 6.79 (d, 2H, J = 9.16 Hz, H$_{arom}$), 3.05 (s, 6H, CH$_3$); ^{13}C NMR (DMSO-d_6, 101 MHz): δ/ppm = 153.4, 151.6, 151.5, 142.1, 140.3, 135.2, 132.9 (2C), 130.7 (2C), 130.3, 128.1 (2C), 127.3, 124.3, 120.1, 119.8, 117.3, 112.2, 112.1 (2C), 105.7, 90.7, 40.0 (2C); MS (ESI): m/z= 390.35 ([M+1]$^+$); Anal. Calcd. for C$_{25}$H$_{19}$N$_5$: C, 77.10; H, 4.92; N, 17.98. Found: C, 77.01; H, 4.79; N, 18.09%.

4.2. Biological evaluation

4.2.1. Cell culture and reference compounds

All cell lines (HL-60, K-562, Z-138, Capan-1, HCT-116, NCI-H460, MM1S, hTERT-RPE-1) were acquired from the American Type Culture Collection (ATCC, Manassas, VA, USA), except for the DND-41 cell line purchased from the Deutsche Sammlung von Mikroorganismen und Zellkulturen (DSMZ Leibniz-Institut, Germany). All cell lines were cultured as recommended by the suppliers. Culture media were purchased from Gibco Life Technologies, USA, and supplemented with 10% fetal bovine serum (HyClone, GE Healthcare Life Sciences, USA). Buffy coat preparations from healthy donors were obtained from the Blood Transfusion Center (Leuven, Belgium). Peripheral blood mononuclear cells were isolated by density gradient centrifugation over Lymphoprep (d = 1.077 g/ml) (Nycomed, Oslo, Norway) and cultured in cell culture medium (DMEM/F12, Gibco Life Technologies, USA) having 8% FBS. Reference inhibitors staurosporine and docetaxel were obtained from Selleckchem (Munich, Germany)). All stock solutions were prepared in DMSO.

4.2.2. Cell proliferation and cytotoxicity assays [35]

Adherent cell lines hTERT RPE-1, Capan-1, HCT-116 and NCI-H460 were seeded at a density between 500 and 1500 cells per well, in 384-well, black walled, clear-bottomed tissue culture plates (Greiner). After overnight incubation, cells were treated with the test compounds at seven different concentrations from 100 to 6.4 x 10^{-3} µM. Suspension cell lines DND-41, MM1S, HL-60, K-562 and Z-138 were seeded at densities ranging from 2500 to 5500 cells per well in 384-well, black walled, clear-bottomed tissue culture plates containing the test compounds at same concentrations. The plates were incubated at 37°C and monitored for 72h in an IncuCyte® device (Essen BioScience Inc., Ann Arbor, MI, USA) for real-time imaging. Images were taken every 3 h, with one field imaged per well under 10x magnification. Cell growth was then quantified based on the

percent cellular confluence as analysed by the IncuCyte® image analysis software. Area under the curve (AUC) values were calculated and used to determine the IC_{50} values. PBMC were seeded at 28000 cells per well in 384-well, black-walled, clear-bottomed tissue culture plates containing the test compounds at the same concentrations. Cells were incubated for 72 hours and were then treated with the CellTiter 96® AQueous Non-Radioactive Cell Proliferation Assay reagent (Promega) according to the manufacturer's instructions. Absorbance of the samples was measured at 490 nm using a SpectraMax Plus 384 (Molecular Devices). The compounds were tested in three independent experiments, which imply PBMC originating from three different donors.

4.2.3. Tubulin immunofluorescence staining

Human cervix carcinoma HEp-2 cells were seeded at 15000c/well in 8-well chamberslides (Ibidi). After an overnight incubation, they were treated with a compound or carrier (DMSO) for 3h and then fixed with 4% PFA, washed and permeabilised. Further treatment was performed according to the standard immunofluorescence procedures and cell nuclei were counterstained with DAPI. Employed antibodies are mouse anti-alpha tubulin (sc-5286, Santa Cruz Biotechnology) and secondary goat anti-mouse IgG conjugated to Alexa Fluor® 488 (A11001, Invitrogen). Images were taken with a Leica TCS SP5 confocal microscope employing a HCX PL APO 63x (NA 1.2)/water immersion objective.

4.2.4. Tubulin Polymerization assay

In vitro tubulin polymerization was carried out using the fluorescence based tubulin polymerization assay (BK011P, Cytoskeleton, Denver, CO) as described by the manufacturer. Briefly, half area 96-well plates were warmed to 37 °C 10 min prior to starting the assay. Test compounds and reference compounds were prepared at 10x stock solutions and added in 5 μl in duplicate wells. Ice-cold tubulin polymerization buffer (2mg/ml tubulin in 80 nM Pipes, 2 mM $MgCl_2$, 0.5 mM EGTA, pH 6.9, and 10μM fluorescent reporter + 15% glycerol + 1 mM GTP) was added into each well, followed by reading with a Tecan Spark fluorimeter in kinetic mode, 61 cycles of 1 reading per minute at 37°C, 4 reads per well (Ex. 350 nm and Em. 450 nm).

4.3. Computational details

The structure of all ligands (**29**, **30**, **41** and **42**) was optimized with the Gaussian 16 software [36] using the M06–2X DFT functional and employing the 6–31+G(d) basis set. To account for the effect of the aqueous solution, during the geometry optimization we included the implicit SMD polarisable continuum model [37] with all parameters for pure water, as employed in many of our

studies concerning various aspects of biomolecular systems [38–40]. This approached identified the most stable conformations of all ligands, considering both *E*- and *Z*-isomers around the central C=C double bond. The results showed the predominant stability of *E*-isomers in all four systems, which were used in the subsequent computational steps, except for a specific case of the most potent system **30**, where both *E*- and *Z*-isomers were considered and discussed in the text. The structure of colchicine was extracted from the non-polymerized colchicine-tubulin crystal structure (5EYP.pdb) and employed as such. Tubulin's β-subunit was pulled out from the complex and prepared for the docking analysis, while both α and β-subunits were used for the visualization of the results, both aspects using the UCSF Chimera program (version 1.12) [41]. The molecular docking studies have been done with SwissDock [42], a web server for docking of small molecules on the target proteins based on the EADock DSS engine, taking into account the entire protein surface as potential binding sites for the investigated ligands.

6. Conflict of interests

The authors declare no conflict of interest.

7. References

1. M. Salahuddin Shaharyar, A. Mazumder, Benzimidazoles: A biologically active compounds, Arab. J. Chem. 10 (2017) 157–173. DOI: 10.1016/j.arabjc.2012.07.017

2. W. Akhtar, M. Faraz Khan, G. Verma, M. Shaquiquzzaman, M. A. Rizvi, S. H. Mehdi, M. Akhter, M. Mumtaz Alam, Therapeutic evolution of benzimidazole derivatives in the last quinquennial period, Eur. J. Med. Chem. 126 (2017) 705–753. DOI: 10.1016/j.ejmech.2016.12.010

3. G. Monika, S. Sarbjot, M. Chander, Benzimidazole: An emerging scaffold for analgesic and anti-inflammatory agents. Eur. J. Med. Chem. 76 (2014) 494–505. DOI: 10.1016/j.ejmech.2014.01.030

4. Yogita Bansal, Om Silakari, The therapeutic journey of benzimidazoles: A review, Bioorg. Med. Chem. 20 (21) (2012) 6208–6236. DOI: 10.1016/j.bmc.2012.09.013

5. A. Rescifina, C. Zagni, M. G. Varrica, V. Pistarà, A. Corsaro, Recent advances in small organic molecules as DNA intercalating agents: Synthesis, activity, and modeling. Eur. J. Med. Chem. 74 (2014) 95–115. DOI: 10.1016/j.ejmech.2013.11.029

6. N. Perin, K. Bobanović, I. Zlatar, D. Jelić, V. Kelava, S. Koštrun, V. Gabelica Marković, K. Brajša, M. Hranjec, Antiproliferative activity of amino substituted benzo[*b*]thieno[2,3-*b*]pyrido[1,2-*a*]benzimidazoles explored by 2D and 3D cell culture system, Eur. J. Med. Chem. 125 (2017) 722–735. DOI: 10.1016/j.ejmech.2016.09.084

7. K. Starčević, M. Kralj, K. Ester, I. Sabol, M. Grce, K. Pavelić, G. Karminski-Zamola, Synthesis, antiviral and antitumor activity of 2-substituted-5-amidino-benzimidazoles, Bioorg. Med. Chem. 15 (2007) 4419–4426. DOI: 10.1016/j.bmc.2007.04.032

8. M. Cindrić, S. Jambon, A. Harej, S. Depauw, M. David-Cordonnier, S. Kraljević Pavelić, G. Karminski-Zamola, M. Hranjec, Novel amidino substituted benzimidazole and benzothiazole benzo[*b*]thieno-2-carboxamides exert strong antiproliferative and DNA binding properties, Eur. J. Med. Chem. 136 (2017) 468–479. DOI: 10.1016/j.ejmech.2017.05.014

9. M. Hranjec, M. Kralj, I. Piantanida, M. Sedić, L. Šuman, K. Pavelić, G. Karminski-Zamola, Novel cyano- and amidino-substituted derivatives of styryl-2-benzimidazoles and benzimidazo[1,2-*a*]quinolines. Synthesis, photochemical synthesis, DNA binding and antitumor evaluation, Part 3. J. Med. Chem. 50 (2007) 5696–5711. DOI: 10.1021/jm070876h

10. K. Brajša, D. Jelić, M. Trzun, I. Zlatar, I. Vujasinović, G. Karminski-Zamola, M. Hranjec, 2D and 3D *in vitro* antitumor activity of amidino substituted benzimidazole and benzimidazo[1,2-*a*]quinolone derivatives. J. Enz. Inh. Med. Chem. 31 (2016) 1139–1145. DOI: 10.3109/14756366.2015.1101093

11. M. Hranjec, G. Pavlović, M. Marjanović, G. Karminski-Zamola, Benzimidazole derivatives related to 2,3-acrylonitriles, benzimidazo[1,2-*a*]quinolines and fluorenes: Synthesis, Antitumor Evaluation *in vitro* and Crystal Structure Determination, Eur. J. Med. Chem. 45 (2010) 2405–2417. DOI: 10.1016/j.ejmech.2010.02.022

12. S.S. Spurr, E.D. Bayle, W. Yu, F. Li, W. Tempel, M. Vedadi, M. Schapira, New small molecule inhibitors of histone methyl transferase DOT1L with a nitrile as a non-traditional replacement for heavy halogen atoms, Bioorg. Med. Chem. Lett. 26 (2016) 4518–4522. DOI: 10.1016/j.bmcl.2016.07.041

13. E. Teodori, S. Dei, A. Garnier-Suillerot, F. Gualtieri, D. Manetti, C. Martelli, M. N. Romanelli, S. Scapecchi, P. Sudwan, M. Salerno, Exploratory chemistry toward the identification of a new class of multidrug resistance reverters inspired by pervilleine and verapamil models, J. Med. Chem. 48 (2005) 7426–7436. DOI: 10.1021/jm050542x

14. Y. Li, J. Wang, C. Pan, F. Meng, X. Chu, Y. Ding, W. Qu, H. Li, C. Yang, Q. Zhang, C. Bai, Y. Chen, Syntheses and biological evaluation of 1,2,3-triazole and 1,3,4-oxadiazole derivatives of imatinib, Bioorg. Med. Chem. Lett. 26 (2016) 1419–1427. DOI: 10.1016/j.bmcl.2016.01.068

15. C. Shang See, M. Kitagawa, P.J. Liao, K. Hee Lee, J. Wong, S.H. Lee, B.W. Dymock, Discovery of the cancer cell selective dual acting anti-cancer agent (*Z*)-2-(1*H*-indol-3-yl)-3-(isoquinolin-5-yl)acrylonitrile (A131), Eur. J. Med. Chem. 156 (2018) 344–367. DOI: 10.1016/j.ejmech.2018.07.011

16. J.J. Li, J. Ma, Y. B. Xin, Z. S. Quan, Y. S. Tian, Synthesis and pharmacological evaluation of 2,3-diphenyl acrylonitriles-bearing halogen as selective anticancer agents, Chem. Biol. Drug. Des. 92 (2018) 1419–1428. https://doi.org/10.1111/cbdd.13180.

17. P. Sanna, A. Carta, M.E. Nikookar, Synthesis and antitubercular activity of 3-aryl substituted-2-[1H(2H)benzotriazol-1(2)-yl]acrylonitriles, Eur. J. Med. Chem. 35 (2000) 535–543. DOI: 10.1016/S0223-5234(00)00144-6

18. J. Das, C.V.L. Rao, T.V.R.S. Sastry, M. Roshaiah, P.G. Sankar, A. Khadeer, M. S. Kumar, A. Mallik, N. Selvakumar, J. Iqbal, S. Trehan, Effects of positional and geometrical isomerism on the biological activity of some novel oxazolidinones, Bioorg. Med. Chem. 15 (2005) 337–343. DOI: 10.1016/j.bmcl.2004.10.073

19. F. Saçzewski, P. Reszka, M. Gdaniec, R. Grünert, P.J. Bednarski, Synthesis, X-ray Crystal Structures, Stabilities, and in Vitro Cytotoxic Activities of New Heteroarylacrylonitriles, J. Med. Chem. 47 (2004) 34383449. DOI: 10.1021/jm0311036

20. V.S. Parmar, A. Kumar, A.K. Prasad, S.K. Singh, N. Kumar, S. Mukherjee, H.G. Raj, S. Goel, W. Errington, M.S. Puar, Synthesis of E- and Z-Pyrazolylacrylonitriles and their Evaluation as Novel Antioxidants, Bioorg. Med. Chem. 7 (1999) 1425–1436. DOI: 10.1016S0968-0896(99)00056-5

21. P. Sanna, A. Carta, M.E. Rahbar Nikookar, Synthesis and antitubercular activity of 3-aryl substituted-2-(1*H*(2*H*)benzotriazol-1(2)-yl)acrylonitriles, Eur. J. Med. Chem. 35 (2000) 535−543. DOI: 10.1016/S0223-5234(00)00144-6

22. A. Carta, P. Sanna, M. Palomba, L. Vargiu, M. La Colla, R. Loddo, Synthesis and antiproliferative activity of 3-aryl-2-(1H-benzotriazol-1-yl)acrylonitriles. Part III, Eur. J. Med. Chem. 37 (2002) 891–900. DOI: 10.1016/S0223-5234(02)01411-3

23. A. Carta, I. Briguglio, S. Piras, G. Boatto, P. La Colla, R. Loddo, M. Tolomeo, S. Grimaudo, A. Di Cristina, R.M. Pipitone, E. Laurini, M.S. Paneni, P. Posocco, M. Fermeglia, S. Pricl, 3-Aryl-2-[1*H*-benzotriazol-1-yl]acrylonitriles: A novel class of potent tubulin inhibitors, Eur. J. Med. Chem. 46 (2011) 4151–4167. DOI: 10.1016/j.ejmech.2011.06.018

24. I. Briguglio, E. Laurini, M.A. Pirisi, S. Piras, P. Corona, M. Fermeglia, S. Pricl, A. Carta, Triazolopyridinyl-acrylonitrile derivatives as antimicrotubule agents: Synthesis, *in vitro* and *in silico* characterization of antiproliferative activity, inhibition of tubulin polymerization and binding thermodynamics, Eur. J. Med. Chem. 141 (2017) 460–472. DOI: 10.1016/j.ejmech.2017.09.065

25. E. M. Silva-García, C. M. Cerda-García-Rojas, R. E. del Río, P. Joseph-Nathan, Parvifoline Derivatives as Tubulin Polymerization Inhibitors, J. Nat. Prod. 82 (4) (2019) 840–849. DOI: 10.1021/acs.jnatprod.8b00860

26. V. Chaudhary, J. B. Venghateri, H. P. S. Dhaked, A. S. Bhoyar, S. K. Guchhait, D. Panda, Novel combretastatin-2-aminoimidazole analogues as potent tubulin assembly inhibitors:

exploration of unique pharmacophoric impact of bridging skeleton and aryl moiety, J. Med. Chem. 59 (2016) 3439–3451. DOI: 10.1021/acs.jmedchem.6b00101

27. W. Zhao, J. K. Bai, H.-M. Li, T. Chen, Y. J. Tang, Tubulin structure-based drug design for the development of novel 4β-sulfur-substituted podophyllum tubulin inhibitors with anti-tumor activity, Sci. Rep. 5 (2015) 10172. DOI: 10.1038/srep10172

28. M. Shaheer Malik, S. A. Ahmed, I. I. Althagafi, M. Azam Ansari, A. Kamal, Application of triazoles as bioisosteres and linkers in the development of microtubule targeting agents, RSC Med. Chem. 11 (2020) 327–348. DOI: 10.1039/C9MD00458K

29. G. Wang, W. Liu, J. Tang, X. Ma, Z. Gong, Y. Huang, Y. Li, Z. Peng, Design, synthesis, and anticancer evaluation of benzophenone derivatives bearing naphthalene moiety as novel tubulin polymerization inhibitors. Bioorg. Chem. 104 (2020) 104265. DOI: 10.1016/j.bioorg.2020.104265

30. H. Chen, L. Miao, F. Huang, Y. Yu, Q. Peng, Y. Liu, X. Li, H. Liu, Glochidiol, a natural triterpenoid, exerts its anti-cancer effects by targeting the colchicine binding site of tubulin, Invest. New Drugs (2020), in print. DOI: 10.1007/s10637-020-01013-1

31. S. Fortin, J. Lacroix, M.-F. Côté, E. Moreau, É. Petitclerc, R. C-Gaudreault, Quick and simple detection technique to assess the binding of antimicrotubule agents to the colchicine-binding site, Biol. Proced. Online 12 (2010) 113–117. DOI: 10.1007/s12575-010-9029-5

32. A. E. Prota, F. Danel, F. Bachmann, K. Bargsten, R. M. Buey, J. Pohlmann, S. Reinelt, H. Lane, M. O. Steinmetz, The novel microtubule-destabilizing drug BAL27862 binds to the colchicine site of tubulin with distinct effects on microtubule organization. J. Mol. Biol. 426 (2014) 1848–1860. DOI: 10.1016/j.jmb.2014.02.005

33. L. Wilson, I. Meza, The mechanism of action of colchicine, J Cell Biol. 58 (1973) 709–719. DOI: 10.1083/jcb.58.3.709

34. N. Perin, S. Škulj, I. Martin-Kleiner, M. Kralj, M. Hranjec, Synthesis and antiproliferative activity of novel 2-substituted N-methylated benzimidazoles and tetracyclic benzimidazo[1, 2-a]quinolines, Polycyclic aromatic compounds 40 (2020) 343–354. DOI: 10.1080/10406638.2018.1441877

35. N. Perin, J. Alić, S. Liekens, A. Van Aerschot, P. Vervaeke, B. Gadakh, M. Hranjec, Different positions of amide side chains on the benzimidazo[1,2-*a*]quinoline skeleton strongly influenced biological activity, New J. Chem. 42 (2018) 7096–7104. DOI: 10.1039/c8nj00416a

36. Gaussian 16, Revision C.01, M.J. Frisch, G.W. Trucks, H.B. Schlegel, G.E. Scuseria, M.A. Robb, J.R. Cheeseman, G. Scalmani, V. Barone, G.A. Petersson, H. Nakatsuji, X. Li, M. Caricato, A.V. Marenich, J. Bloino, B.G. Janesko, R. Gomperts, B. Mennucci, H.P. Hratchian, J.V. Ortiz, A.F. Izmaylov, J.L. Sonnenberg, D. Williams-Young, F. Ding, F. Lipparini, F. Egidi, J. Goings, B. Peng, A. Petrone, T. Henderson, D. Ranasinghe, V.G. Zakrzewski, J. Gao, N. Rega, G. Zheng, W. Liang, M. Hada, M. Ehara, K. Toyota, R. Fukuda, J. Hasegawa, M. Ishida, T. Nakajima, Y. Honda, O. Kitao, H. Nakai, T. Vreven, K. Throssell, J.A. Montgomery Jr., J.E. Peralta, F. Ogliaro, M.J. Bearpark, J.J. Heyd, E.N. Brothers, K.N. Kudin, V.N. Staroverov, T.A. Keith, R. Kobayashi, J. Normand, K. Raghavachari, A.P. Rendell, J.C. Burant, S.S. Iyengar, J. Tomasi, M. Cossi, J.M. Millam, M. Klene, C. Adamo, R. Cammi, J.W. Ochterski, R.L. Martin, K. Morokuma, O. Farkas, J.B. Foresman, D.J. Fox, Gaussian, Inc., Wallingford CT, 2016

37. A.V. Marenich, C.J. Cramer, D.G. Truhlar, Universal Solvation Model Based on Solute Electron Density and on a Continuum Model of the Solvent Defined by the Bulk Dielectric Constant and Atomic Surface Tensions. J. Phys. Chem. B 113 (2009) 6378–6396. DOI: 10.1021/jp810292n

38. T. Tandarić, R. Vianello, Computational Insight into the Mechanism of the Irreversible Inhibition of Monoamine Oxidase Enzymes by the Antiparkinsonian Propargylamine Inhibitors Rasagiline and Selegiline. ACS Chem. Neurosci. 10 (2019) 3532–3542. DOI: 10.1021/acschemneuro.9b00147

39. I. Perković, S. Raić-Malić, D. Fontinha, M. Prudêncio, L. Pessanha de Carvalho, J. Held, T. Tandarić, R. Vianello, B. Zorc, Z. Rajić, Harmicines - Harmine and Cinnamic Acid Hybrids as Novel Antiplasmodial Hits. Eur. J. Med. Chem. 187 (2020) 111927. DOI: 10.1016/j.ejmech.2019.111927

40. A. Maršavelski, R. Vianello, What a difference a methyl group makes - the selectivity of monoamine oxidase B towards histamine and *N*-methylhistamine. Chem. Eur. J. 23 (2017) 2915–2925. DOI: 10.1002/chem.201605430

41. E.F. Pettersen, T.D. Goddard, C.C. Huang, G.S. Couch, D.M. Greenblatt, E.C. Meng, T.E. Ferrin, UCSF Chimera - A Visualization System for Exploratory Research and Analysis. J. Comput. Chem. 13 (2004) 1605–1612. DOI: 10.1002/jcc.20084

32. A. Grosdidier, V. Zoete, O. Michielin, SwissDock, a protein-small molecule docking web service based on EADock DSS. Nucleic Acids Res. 39 (2011) W270–W277. DOI: 10.1093/nar/gkr366

GRAPHICAL ABSTRACT
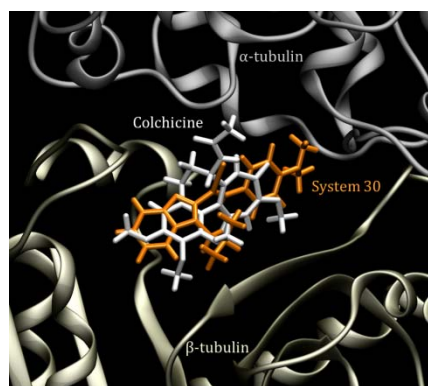
HIGHLIGHTS

• novel *N*-substitted benzimidazole based acrylonitriles

• selective antiproliferative activity in submicromolar range of concentrations (IC$_{50}$ 0.2 – 0.6 µM)

• mechanism of biological action demonstrated inhibition of the tubulin polymerization

• NMe$_2$ group on the phenyl unit promotes binding by allowing interactions with Lys352

• *N*-isobutyl group occupies hydrophobic pocket and ensures a correct ligand orientation